의학박사 학위논문

Role of TASK-2 channel in B lymphocytes

B림프구에서 TASK-2 이온통로의 역할

2013년 8월

서울대학교 대학원

의학과 생리학 전공

신 동 훈

A thesis of the Degree of Doctor of Philosophy

Role of TASK-2 channel in B lymphocytes

B 림프구에서 TASK-2 이온통로의 역할

August, 2013

The Department of Physiology,

Seoul National University

College of Medicine

Dong Hoon Shin

B림프구에서 TASK-2 이온통로의 역할

Role of TASK-2 channel in B lymphocytes

지도교수 김 성 준

이 논문을 의학박사 학위논문으로 제출함

2013년 7월

서울대학교 대학원

의학과 생리학 전공

신 동 훈

신동훈의 의학박사 학위논문을 인준함

2013년 7월

위 원 장 박 종 안 (인)

부위원장 김 성 준 (인)

위 원 남 주 현 (인)

위 원 예 상 규 (인)

위 원 장 은 화 (인)

Role of TASK-2 channel in B lymphocytes

B림프구에서 TASK-2 이온통로의 역할

by

Dong Hoon Shin

A thesis submitted to the Department of Medicine in partial fulfillment of the requirements for the Degree of Doctor of Philosophy in Medical Science (physiology) at Seoul National University College of Medicine

July 2013

Approved by Thesis Committee:

Professor Park, Sung Wan Chairman
Professor Kim, Sung Joon Vice chairman
Professor Nam, Joo Hyun
Professor Ye, Sang-Kyu
Professor Zhang, Yin-hua

ABSTRACT

Stimulation of B cell receptors (BCR-ligation) induces apoptosis in immature B cells, which is critical for the elimination of self-reactive clones. On the other hand differentiation of B lymphocytes occurs in spleen and lymph node where O_2 tension is physiologically hypoxic (1-5% P_{O2}). K^+ channels play critical roles in apoptosis and cell volume in a variety of cells including lymphocytes. However, responses of K^+ channel activity to BCR-ligation and to sustained hypoxia (SH, 3% $P_{O2,}$ 24 h) stimulation are unknown yet.

In this study, I found remarkable increase of voltage-independent background-type K^+ conductance in mouse immature B cell line (WEHI-231) 24 h after BCR-ligation. The biophysical properties (unitary conductance and pH-sensitivity) of the upregulated K^+ channel were consistent to those of TASK-2, a member of two-pore domain K^+ (K2P) channel family. The expression of TASK-2 and its upregulation by BCR-ligation was confirmed by RT-PCR, immunoblot assay, and by TASK-2 specific siRNA transfection (siTASK-2). The BCR-ligation induced increase of K^+ current was prevented by

calcineurin inhibitors (cyclosporine A or FK506). Transfection with siTASK-2 attenuated the apoptosis of WEHI-231 caused by BCR-ligation. TASK-2 activity and its mRNA were also confirmed in the primary splenic B cells of mouse.

Similar to BCR-ligation, SH condition also increased TASK-2 channel activity in WEHI-231 cells. The increase of K^+ conductance was observed from 20 h of hypoxia and sustained up to 48 h. The hypoxic upregulation of TASK-2 was prevented by pretreatment with 10 μM YC-1, known as an inhibitor of hypoxia inducible transcription factor-1 (HIF-1α). Consistently, siHIF-1α transfection attenuated the hypoxic upregulation of TASK-2 current, whereas TASK-2 current was increased in sh-HIF-1α expressing WEHI-231 cells under 24–36 h control cultured condition. In addition, SH exposed WEHI-231 cells showed augmentated $[Ca^{2+}]_c$ increase in response to BCR-ligation. The expression of TASK-2 and their upregulation by SH condition was also observed in the primary splenic B cells from mice.

In summary, TASK-2 channels in B lymphocytes are upregulated by both BCR-ligation and SH condition. It is proposed that TASK-2 channels play multiple roles depending

on the context of stimuli. Under the BCR-ligation, membrane hyperpolarization and excessive K^+ efflux via TASK-2 might contribute to apoptotic volume decrease. On the other hand, the hypoxic upregulation of TASK-2 also augments Ca^{2+} signaling that is critical for the fate and activity of B lymphocytes.

Keywords: B lymphocyte, TASK-2 channel, Hypoxia, BCR-ligation

Student number: 2008-21944

CONTENTS

LIST OF TABLES AND FIGURES

Chapter 1

Chapter 2

LIST OF ABBREVIATIONS

LK_{bg} : Large-conductance background K^+ channels

MK_{bg} : Medium-conductance background K^+ channels

BCR-ligation : Cross-linking membranous IgM-type B cell receptors

SH : Sustained hypoxia

K_v : Voltage-gated K^+ channels

K2P : Two-pore domain K^+ channels

K_{bg} : Background K^+

NFAT : Nuclear factor of activated T cells

AVD : Apoptotic volume decrease

HIF-1α : Hypoxia Inducible Factor-1 alpha

NT : Normal Tyroide's solution

sh-HIF-1α : stably express hypoxia-activated HIF-1α mutant

INTRODUCTION

B lymphocytes are responsible for specific humoral immune response to pathogens Differentiation of B lymphocyte starts from pluripotent stem cells located in bone marrow through the process of developmental stage. The maturation of B lymphocytes is completed in the secondary lymphoid organs such as lymph nodes and spleen.

During the development in bone marrow, elimination of autoreactive clones of B lymphocytes is crucial to prevent autoimmune disease (Kuppers et al., 1999). It is widely accepted that the activation of K^+ and Cl^- channels is the primary event of apoptosis to induce apoptotic volume decrease (AVD) since shrinkage of cell volume is often observed during the early stages of apoptosis. The depletion of intracellular K^+ has been suggested to play key roles in the early process of apoptosis (Bortner et al., 2007; Lang et al., 2007). In this respect, the identity of K^+ channels and its regulation by BCR-ligation is an intriguing theme to investigate the apoptosis of immuature B cells. Experimentally, B cell stimulation is achieved by cross-linking membranous IgM-type B cell

receptors (BCR-ligation) using anti-IgM antibody (αIgM). Since apoptosis after BCR-ligation typically takes more than several hours to days, it is possible to hypothesize that persistent K^+ channel upregulation occurs under BCR-ligation. However, such possibility has rarely been investigated in immature B lymphocytes.

Role of K^+ channel in lymphocytes

K^+ channels play key roles in setting the negative resting membrane potential and ion homeostasis of cells. This negative membrane potential is critical for the physiological and immunological responses of lymphocytes by providing electromotive forces for Ca^{2+} influx and cell volume regulation. Of the various K^+ channels, voltage-gated K^+ channels such as $K_v1.3$ and intermediate conductance Ca^{2+}-activated K^+ channels (SK4/IKCa1), are regarded to be major players in lymphocytes (Cahalan et al., 2009). Related to differentiation of lymph node, in case of nascent naïve B lymphocytes, although currents of $K_v1.3$ and IKCa1 are reduced, they increased, differentiating into receptor editing and memory B lymphocytes (Wulff et al., 2004). However, as indicated by their names, the contributions made by $K_v1.3$ and IKCa1 require membrane

depolarization and an elevated $[Ca^{2+}]_c$, respectively.

Recently, background-type K^+ (K_{bg}) channels with voltage-independent activity have drawn attention as potential regulators of immune cell function (Meuth et al., 2008; Pottosin et al., 2008; Bittner et al., 2009). These channels belong to the two-pore domain K^+ (K2P or KCNK) channel family. The K2P channels consist of dimeric complex of four transmembrane domains with two pore domains. Due to their 'background' or 'leak' activity, K2P channels are believed to play pivotal roles in the establishment of resting membrane potential in various cell types. In addition, K2P channel members display sensitivities to a number of physiochemical stimuli, such as, membrane stretch, temperature, and pH (Kim et al., 2005; Bayliss et al., 2008).

K2P channel in B lymphocytes

It has been demonstrated that two types of K_{bg} channels with distinctive unitary conductance are expressed in mouse B cells. First, the channel with slope conductance of 300 pS under divalent cation-free (DVF) conditions was identified as TREK-2 (Zheng et al., 2009). Second, the channel with slope

conductance of 112 pS was named as medium conductance background K^+ channel (MK_{bg}, Nam et al., 2007).

The TREK subfamily members of K2P channels are activated to arachidonic acid and membrane stretch (Duprat et al., 2007; Kim et al., 2005). In B cells, Ca^{2+} influx through arachidonic acid-activated cation channels is actually augmented by membrane hyperpolarization induced by the concomitant activation of TREK-2 (Zheng et al., 2008). However, in contrast to TREK-2, neither the molecular nature nor the physiological properties of MK_{bg} have been elucidated.

Hypoxia and lymphocytes

The secondary lymphoid organs (e.g. especially subcortical layers of spleen) are intrinsically hypoxic (1-5% P_{O2}), and the physiological hypoxia has been reported to play a key role in differentiation of B lymphocytes. Oxygen pressure increases to the highest near the splenic artery, lymph node and gradually deceases with distance from the artery (Caldwell et al., 2001; Huang et al., 2007). In addition, immune cell are often exposed to anoxia under pathological condition such as poorly perfused atherosclerotic regions (Sluimer et al., 2008).

Hypoxia is known to modulate a variety of immune responses. In T lymphocytes, prolonged hypoxia impaires cytokine production and inhibites T lymphocytes differentiation (Zuckerberg et al., 1994). In addtion, migration of dendritic cells to peripheral lymph node is also known to be impaired when exposesed to hypoxia (Mancino et al., 2008). However, in B lymphocytes, chronic hypoxic conditions (e.g. high altitude) appeared to enhance the humoral immune reactivity, i.e. production of immunoglobulins (Singh et al., 1977).

Although the influence of O_2 tension to immunological responses has been widely investigated, hypoxic regulation of ion channels in immune cells has been rarely studied. In T lymphocytes, exposure to acute hypoxia (AH; 15 min, 1% O_2) inhibits $K_v1.3$ current. In addition, decrease of $K_v1.3$ expression was observed in T lymphocytes undergoing sustained hypoxia (SH; 24 h, 1% O_2) condition. Inhibition of K_v channels induces membrane depolarization and suppresses the activation response of T lymphocytes (Conforti et al., 2003; Szigligeti et al., 2006; Chimote et al., 2012). Hypoxia regulates various functions of immune cells such as T cells via hypoxia inducible factor-1 alpha (HIF-1α)(McNamee et al., 2013). However,

regulation of ion channels by hypoxia in B lymphocytes remain explored.

Goals of the study

In pilot studies, I found that the K_{bg} channel activities were increased by both BCR-ligation and by SH conditions. Base on these results, I went on and analysed the mechanisms and functions of K^+ channel activity in mouse B cell line (WEHI-231 cells) in response to BCR-ligation (αIgM, 12 h) and to SH (3% P_{O2}, 24 h). Main goals of this study are to identify the molecular nature of the upregulated K^+ channel(s), and physiological implication of the augmented K^+ channel activity in B lymphocytes.

MATERIALS AND METHODS

1. Cell culture and mouse B cell isolation

WEHI-231 cells (American Type Culture Collection, Manassas, VA, USA) were grown in Dulbecco's modified Eagle's medium (DMEM; Gibco Invitrogen, Grand Island, NY, USA) supplemented with 10% (v/v) fetal bovine serum (Invitrogen, Carlsbad, CA USA), 50 μM 2-mercaptoethanol (Sigma, St. Louis, MO), and 1% penicillin/streptomycin (Invitrogen) at 37 ℃ in 20% O_2/10% CO_2 (control condition) and 3% O_2/10% CO_2 (SH condition).

The total population of mouse primary B cells was prepared from the spleens of 6-week-old C57BL/6 mice. Mice were sacrificed using 100% CO_2, and the spleens were removed immediately. The spleens were dissociated into single cell suspensions and B cells were isolated using Spin-Sep^{TM} B cell enrichment kits (Stem Cell Technologies, Vancouver, BC, Canada). Isolated B cells were kept in AIM-V medium (Invitrogen) supplemented with 10% (v/v) fetal bovine serum at 37 ℃ in control and SH conditions.

2. Plasmids and gene transfection

The mammalian expressible plasmid for mouse KCNK5 was purchased from Openbiosystems (Alabama, USA). The mKCNK5 cDNA sequence was verified by nucleotide sequencing, and was identical to a registered sequence (Genbank Accession NM_021542.4). mKCNK5 siRNA, a mixture of four siRNAs against mKCNK5, was purchased from Dharmacon (Lafayette, USA) and mHIF-1α siRNA was purchased from Santa Cruz Biotechnology (Santa Cruz, CA, USA). The Pro-Ser-Thr-rich oxygen-dependent degradation domain (ODDD) determines the protein stability of HIF-1α, and O_2-stable form of HIF-1α cDNA (sh-HIF-1α) (obtained from Dr. Park, Jong-Wan) was generated by deleting 3 degradation motifs (aa's 397-405, 513-553, and 554-595) (Yeo et al., 2006). Plasmids and siRNAs were transiently transfected a nucleofector and corresponding kit (AMAXA Biosystems, Cologne, Germany). Briefly, WEHI-231 cells were resuspended in nucleofector solution, and 100 μl of cells (2×10^6 to 5×10^6 /ml) were mixed with 1 μg of pmax green fluorescent protein (GFP) vector and siRNA (200 nM), transferred to a cuvette, and nucleofected with AMAXA nucleofector. The cells

transfected with scRNA (Invitrogen) were used as negative controls.

3. Electrophysiology

Cells were transferred into a bath mounted on the stage of a IX-70 inverted microscope (Olympus, Osaka, Japan). The bath (~0.15 ml) was superfused at 5 ml/min and voltage clamp experiments were performed at room temperature (22-25° C). Patch pipettes with a free-tip resistance of 2.5–3.5 MΩ were connected to the head stage of an Axopach-1D patch-clamp amplifier (Molecular Devices, Sunnyvale, CA, USA). pCLAMP software v.9.2 and a Digidata-1322A (Molecular Devices) were used to acquire data and apply command pulses. Throughout the w-c clamp experiments, 3 mM MgATP was included in the pipette solution to minimize the influence of the activity of LK_{bg}/TREK-2 (Nam et al., 2004).

Single channel activities were recorded at 10 kHz in cell-attached (c-a) and inside-out (i-o) configurations. Voltage and current data were low-pass filtered at 1 kHz. Current traces were stored and analyzed using Clampfit v.9.2 and Origin v.7.0 software (OriginLab, Northampton, MA, USA). Single

channel recordings were analyzed to obtain amplitude histograms and total channel activities (np_o) where n and p_o are the observed level of channel opening and the open probability, respectively.

The names and compositions of the experimental solutions used in the electrophysiological experiments are listed in Table 1.

4. Western blot

WEHI-231 cells were incubated hypoxia for different times. For control experiments, mouse TASK-2 transfected HEK293T cells were also prepared. Antibodies against TASK2 (APC-037, Alomone Labs, Jerusalem, Israel), β-tubulin (2146S, Cell Signaling Technology, Beverly, MA, USA) and GAPDH (Sc-20357, Santa Cruz Biotechnology, Santa Cruz, CA, USA) were purchased from commercial sources.

WEHI-231 cells were biotinylated using the membrane impermeable Sulfo-NHE-SS-Biotin (Pierce, Rockford, IL, USA) in phosphate buffered saline (PBS) was added to the cell suspension and gently shaked for 1 hrs at 4℃. After quenching free biotin by the addition of 50 mM Tris-Cl (pH 7.4), WEHI-

231 cells were lysed in lysis buffer (0.5 M EDTA, 25 mM Tris-Cl pH 7.4, 150 mM NaCl, 1% Triton X-100) and centrifuged at 13,000 g for 10 min. Supernatents were incubated with solution containing NeutrAvidin agarose resins (Pierce, Rockford, IL, USA) for 1 h at room temperature. Beads were washed two times with 0.1% Tris buffered saline-Tween (TBS-T). Avidin binding proteins were eluted with elution buffer [62.5 mM Tris-Cl pH 6.8, 1% sodium dodecyl sulfate (SDS), 10% glycerol, 50 mM dithiothreitol (DTT)] and immunoblotting was performed using a conventional procedure. To obtain total proteins, cells were harvested and suspended in homogenization buffer (0.5 M EDTA, 25 mM Tris-Cl pH 7.4, 150 mM NaCl, 1% Triton X-100, 1 mM $NaVO_4$, and 1 mM β-glycerophosphate) containing a complete protease inhibitor mixture (Roche Applied Science, Mannheim), and lysed using a 22-gauge needle. Cell debris was then removed by centrifugation, and the cleared lysates were mixed with recovered in SDS sample buffer and were separated using 4-12% precast poly-acrylamide gels. The separated proteins were transferred to nitrocellulose membranes, which were blocked by incubating for 1 h in a solution containing 5% BSA in

20 mM Tris-HCl (pH 7.5), 150 mM NaCl, and 0.05 % Tween-20. Membranes were then incubated with the appropriate primary and secondary antibodies, and protein bands were detected using enhanced chemiluminescence. Membranes were then stripped for 30 min in stripping buffer (60 mM Tris-HCl, pH 6.8, 100 mM 2-mercaptoethanol, 2% SDS) and re-probed with β-tubulin or GAPDH antibody.

6. RT-PCR

Total RNA was isolated from WEHI-231 cells using TRizol (Invitrogen, Carlsbad, CA, USA). Mouse TASK-1, TASK-2, TASK-4, TASK-5, HIF-1α mRNA, 18s rRNA and GAPDH were analyzed by RT-PCR. One microgram of RNA were reverse transcribed at 48℃ for 20 min, and the cDNAs produced were amplified over 30 PCR cycles (60℃ for 1 min, 72℃ for 2 min, and 95℃ for 45 s). PCR products (5 μl) were electrophoresed on a 2% agarose gel at 100 V in a 1 x Tris-acetate-EDTA buffer and visualized using ethidium bromide. The nucleotide sequences of the primers used are summarized in Table 2.

7. Flow cytometry

Following the transfection of WEHI-231 cells with scRNA or siTASK-2, cells were incubated with αIgM for 48 h. They were then washed twice with cold PBS and suspended in Binding Buffer (556454, BD Pharmingen, San Jose, CA, USA), and diluted to 10^6 cells/ml. 1 ml of these suspensions were transferred to 5 ml polystyrene round-bottom tubes and added by 5 μl Annexin V-FITC (556419, BD Pharmingen) and 5 μl 7AAD-PE (559925, BD Pharmingen). The tubes were then gently vortexed and incubated in the dark for 15 minutes at RT (25℃). 400 μl of the Binding Buffer was added to each of the tubes before analysis using FACS Calibur (BD Bioscience, San Jose, CA, USA).

8. Ca^{2+} measurement

WEHI-231 cells were loaded with fura-2 acetoxymethyl ester (5 μM, 30 min, room temperature) and washed twice with fresh NT (145 mM NaCl, see table 1.) or High K^+ (replace 145 mM NaCl with 145 mM KCl) solutions. The Fura-2 loaded cells were transferred into a microscope stage bath (approximately 100 μl) mounted on the stage of an inverted microscope (IX 70;

Olympus) and perfused with HEPES buffered NT solution at 5 ml/min. Fluorescence was monitored using a Polychrome IV monochromator (TILL Photonics, Martinsried, Germany), a Cascade 650 CCD camera (Roper Scientific, Sarasota, FL, USA) and Metafluor software (Universal Imaging, Downingtown, PA, USA) at excitation wavelengths of 340 and 380 nm, and an emission wavelength of 510 nm. At the end of each experiment, Ca^{2+}-free solution with 5 mM EGTA were applied to produce a minimum fluorescence ratio (R_{min}; 340/380 nm). Then, 2 μM ionomycin and 10 mM $CaCl_2$ were applied to confirm a maximum ratio of fluorescence (R_{max}; 340/380 nm). The ratio values of $[Ca^{2+}]_{ratio}$ were calculated as;

$[Ca^{2+}]_{ratio} = (R340/R380 - R_{min})/R_{max.}$

9. Statistical analysis

Data are expressed as mean ± SEM. Student's t-test and ANOVA was used to test for significance at the level of < 0.01 or 0.05.

RESULTS

Part 1. BCR-ligation induced TASK-2 K^+ channel in B lymphocytes

At first, the whole-cell (w-c) currents of control and αIgM treated WEHI-231 cells were compared (Fig. 1). Ramp-like depolarization from -90 to 60 mV was applied to obtain current to voltage relations (I/V curve). Original I/V curves from individual cells are shown as superimposed traces (Fig. 1B). In the control group, the membrane conductance (slope of the I/V curve at negative membrane voltages) was relatively low, and prominent background K^+ conductance was rarely observed (Fig. 1A, B, left panels). The membrane conductance tended to increase with a reversal potential close to -80 mV, and the change became prominent during the 6 h. The I/V curves of B cells were collected between 9-15 h after BCR-ligation (12 h-αIgM, Fig. 1A and B, middle panels), and I/V curves were also obtained after 24-30 h of BCR-ligation (24 h-αIgM). Averaged I/V curves showed that leak-type K^+ conductance prominently increased in 12 h-αIgM cells, and this change was reversed to the control level the following day (Fig. 1A). The

I/V curves of 12 h-αIgM WEHI-231 showed a weak inward rectification at voltages above 20 mV. The linear membrane conductance of 12 h-αIgM cells at negative voltages indicate the increased activity of K_{bg} channels. Consistent with the increased numbers of K_{bg} channels, almost linear I/V curves with reversal potential at 0 mV were observed under symmetrical K^+ conditions (145 mM KCl on both sides of the plasma membrane) in 12 h-αIgM cells (Fig. 1C).

To elucidate specific types of K_{bg} channels induced by BCR-ligation, single channel properties were investigated. In the c-a patch clamp under a symmetrical K^+ condition (DVF High K^+ solution, Table 1), ion channels with burst type activity were observed at negative membrane voltage (-60 mV) more frequently in 12 h-αIgM than in control cells (Fig. 2A, B, n=11). In the i-o patch conditions with symmetrical high K^+ solutions, the voltage-dependence of single channel currents showed weak inward rectification with an unitary conductance of 112 pS (DVF pipette solution) or 78 pS (Ca^{2+} and Mg^{2+} containing high K^+ pipette solution) at negative voltages (Fig. 2C, D). The slope conductance and voltage-independent activity at negative voltages were consistent with the

properties of MK_{bg}, which has been previously described in WEHI-231 cells (Nam et al., 2004).

When I compared with the reported characteristics of K2P channels, the relatively large unitary conductance (78 pS with physiological Ca^{2+} and Mg^{2+}) and burst-like activity of MK_{bg} were similar to those of TASK-2 (70 pS at -60 mV) (Kim et al., 2005; Lotshaw et al., 2007). Therefore, I tested the sensitivity of w-c current to extracellular pH (pH_e) changes in 12 h-αIgM cells, and compared this with the responses of mouse TASK-2 (mTASK-2) overexpressed HEK293T cells (Fig. 3). Here, the holding voltage was kept at 20 mV to induce the inactivation of K_v channels. In 12 h-αIgM cells, the non-inactivating background outward current was increased by alkaline pH_e and decreased by acidic pH_e with half-activation pH_e at 7.4 (Fig. 3A, B, n=7). The pH_e-dependence was similar to that of mTASK-2 current (IC_{50}=7.5) in HEK293T cells (Fig. 3C, D, n=9).

The pH_e-sensitivity of MK_{bg} in WEHI-231 was also tested under o-o patch clamp conditions, and compared with that of mTASK-2 in HEK-293 (Fig. 4A, B, n=6). The pH_e-sensitivities of MK_{bg} and mTASK-2 were found to be similar

(Fig. 4B), as were their slope conductance values. The average conductance of mTASK-2 recorded under i-o conditions was 65 pS (Fig. 4D, n=5).

RT-PCR analysis demonstrated the expression of TASK-2 mRNA in WEHI-231 cells, while other TASK-1, 3, 5 and TALK-1 were not found (Fig. 5A). An immunoblot study using TASK-2 specific antibody also confirmed the expression of TASK-2 protein and its upregulation by BCR-ligation in WEHI-231 cells (Fig. 5B, C, n=4).

Based on the above results, I could conclude that TASK-2 corresponds to MK_{bg} in WEHI-231 cells, and that the expression of TASK-2 is significantly increased by BCR-ligation. Several signalling mechanisms, such as, the PLCγ2/calcineurin and the NFκB pathways have been investigated with respect to involvement in B cell apoptosis in WEHI-231 cells (Eeva et al., 2004). Interestingly, the upregulation of MK_{bg} by αIgM was inhibited by the co-treatment with cyclosporine A or FK506, both calcineurin inhibitors (Fig. 6A, B, n=8, 13). In contrast, the treatment with the NFκB inhibitor, Bay 11-7082 (10 μM), did not affect the upregulation of MK_{bg}/TASK-2 by BCR-ligation (Fig. 6C,

n=16).

Then it was tested whether the increased TASK-2 activity is involves in the apoptosis of WEHI-231 cells. Because no specific pharmacological blocker of TASK-2 was available yet, TASK-2 specific siRNA (siTASK-2) was used. The siTASK-2 was transfected into WEHI-231 48 h before BCR-ligation. TASK-2 downregulation was confirmed by immunoblot assay (Fig 7A). In the w-c patch clamp recordings of pH_e-sensitive currents (Fig. 7B, n=14). WEHI-231 cell death was then evaluated by flow cytometry using Anexin V-FITC and 7AAD-PE at 48 h after BCR-ligation. As shown in Fig. 7, the proportion of Annexin-V (+) or 7AAD (+) cells increased significantly by BCR-ligation, and the proportion of cell death was lower in siTASK-2 transfected cells as compared with scRNA transfected cells (Fig. 8).

Finally, I examined whether TASK-2 is also expressed in primary B cells isolated from mouse spleen. In the w-c patch clamp experiments, I found that a proportion of splenic B cells (5 of 22 trials) express K_{bg} current with pH_e-sensitivity that is activated by alkaline pH_e (Fig. 9A). The o-o patch clamp recordings of splenic B cells also demonstrated pH_e-sensitive

K^+ channels (Fig. 9B, n=6).

Furthermore, the amplitude of pH_e-sensitive K^+ channel at 0 mV with NT bath solution (1.3-1.5pA) was consistent with the expected amplitude of TASK-2 under the same ionic conditions. Also, RT-PCR analysis of splenic B cells revealed the expression of TASK-2 transcripts (Fig. 9C).

Part 2. Hypoxia induced TASK-2 K^+ channel in B lymphocytes

In w-c configuration, cells were held at -60 mV, and ramp-like depolarization pulses (from -100 to 100 mV) were applied to obtain I/V curves. Under atmospheric O_2, basal w-c currents in control WEHI-231 cells showed outwardly rectifying K^+ current (K_v) that was activated from depolarizing voltages (>-20 mV). In contrast, sustained hypoxia (SH, 3% P_{O2}, 24 h) induced prominent outward K^+ current with voltage-independent background activity (K_{bg}; Fig. 10A). In the WEHI-231 cells exposed to SH (SH cells), the reversal potential of I/V curve was close to -80 mV, which was close to the K^+ equilibrium potential, indicating that K_{bg} is the main ion channel that would set the hyperpolarized membrane potential. Replacing extracellular Na^+ with equimolar K^+ revealed a large inward current at negative voltages, consistent with the increased K_{bg} activity (Fig. 10B).

The increase of K_{bg} current during hypoxia showed a bi-phasic pattern in its time course, with an initial transient increase at around 4 h and a further increase from 16-24 h and

a slight decline at 48 h (Fig. 10C). The peak K_{bg} was observed at 24 h.

Since the above patch clamp study of SH cells was performed under ambient P_{O2}, we also tested the effect of acute hypoxia (AH) by superfusing with 100% N_2-bubbled NT solution. I confirmed that the P_{O2} of perfusate in bath was lowered to 1-2% on changing to the N_2-saturated solution (data not shown), and the AH immediately decreased the amplitude of K_v current of control WEHI-231 cells (Fig. 10D, n=6). In contrast, however, the K_{bg} currents measured in SH cells was increased by AH (Fig. 10E, n=9). Paired comparison of AH-induced changes in current amplitudes more clearly demonstrated the differential responses of control and SH cells to AH (Fig. 10F). In each cell, normalized current amplitudes at -20 mV (for comparison of mainly K_{bg} activity) and 20 mV (for comparison of both K_{bg} and K_v activities) showed that the K_{bg} at negative voltage was increased by AH in SH cells.

Mouse B cells express TREK-2 and TASK-2, two members of the K2P (KCNK) family (Zheng et al., 2009; Nam et al., 2011). Since TREK-2 channels are effectively activated by arachidonic acid (AA), amplitudes of 10 μM AA-activated K^+

current at negative membrane voltage in the symmetrical KCl conditions were compared between control and SH cells. The AA-activated TREK-2 current was obtained by digital subtraction of initial I/V curve (control) or 10 s AA-treated I/V curve (SH) from the steady-state (120 s) I/V curve. A large increase in the slope of I/V curve was similarly observed in both control and SH cells (Fig. 11A, B).

Single channel activities of AA-activated TREK-2 were also compared in c-a recording. With symmetrical KCl solutions, 10 μM AA activated K_{bg} channels with relatively large conductance (17 pA at −60 mV) in both control and SH cells. The calculated maximum activity (NP_o) of TREK-2 with 10 μM AA was not different between control and SH cells (Fig. 11C, D).

I next investigated the single channel properties of SH-induced K_{bg} channels in the c-a recording with symmetrical KCl solutions. In SH cells, inward K^+ channel current with 5.5 pA amplitudes at −60 mV were frequently observed (Fig. 11E bottom panel), which was consistent with the known unitary conductance of TASK-2 channel in B cells (La et al., 2006). In control cells, however, the inward K^+ channel current was rarely observed (Fig. 11E upper panel). In total, the TASK-2-

like channel activity (NPo) was markedly higher in SH cells (Fig. 11F, n=6).

The hallmark property of TASK-2 is the pH_e sensitivity (Reyes et al., 1998). While the changes of pH_e had an insignificant effect on K_v current in control cells (Fig. 12A), the K_{bg} current in SH cells was significantly augmented and inhibited at pH_e 8.4 and 6.4, respectively (Fig. 12B). The pH_e-sensitive outward K_{bg} current was rarely observed in the control cells. The summarized current amplitudes at -20 mV are shown in the bar graph depicted in Fig 12C (n=10).

An immunoblot assay using the mouse TASK-2 specific antibody confirmed the expression of TASK-2 in WEHI-231 cells. Protein samples were also obtained from mTASK-2 overexpressed in HEK-293T cells as a positive control. TASK-2 total protein expression significantly increased in SH cells (Fig. 13A, upper panel). In addition, a surface biotinylation assay demonstrated that the membrane expression of TASK-2 was definitely increased in SH cells (Fig. 13A, lower panel). The normalized membrane and total TASK-2 expression (TASK-2/β-tubulin) were significantly increased in the SH cells (Fig. 13B, n=4).

The molecular identity of hypoxia upregulated K^+ channel as TASK-2 was further proven by TASK-2 specific siRNA (siTASK-2) transfection. Scrambled siRNA (scRNA) or siTASK-2 was co-transfected with GFP vector in WEHI-231 cells. Twenty four hours after the transfection, the two groups of cells were further incubated under hypoxia (24 h, 3% P_{O2}) conditions. We then performed whole cell patch clamp in the GFP-positive cells under fluorescence microscopy examination. The representative I/V curve of scRNA transfected cells consistently showed K_{bg} current, while siTASK-2 transfected cells hardly showed a K_{bg} current (Fig 14A). To further rule out the influence from K_v current, the holding voltage was fixed at 20 mV that induced full inactivation of K_v channels. A reverse ramp pulse from 100 to -100 mV was applied to obtain an I/V curve of non-inactivating K_{bg} current. The scRNA transfected cells consistently demonstrated increased K_{bg} currents, which was not observed in the siTASK-2 transfected cells (Fig 14B, n=12).

Many adaptive cellular responses to hypoxia are mediated by HIF-1. HIF-1 functions as a heterodimer, consisting of HIF-1α and HIF-1β (Semenza et al., 1996; Nizet et al., 2009).

The knockdown of HIF-1α expression by transfection of mouse HIF-1α specific siRNA markedly decreased HIF-1α mRNA in WEHI-231 cells (Fig. 15A). In the w-c clamp experiment, reverse ramp pulse from 100 to -100 mV (holding voltage, 20 mV) was applied to obtain an I/V curve of K_{bg}. SH-induced TASK-2 current was inhibited by siHIF1α but not by scRNA (Fig 15B, n=13). *Vice versa*, overexpression with O_2-stable sh-HIF-1α alone induced TASK-2 in WEHI-231 cells under control culture conditions (Fig. 15C, n=10). YC-1 is a HIF-1 inhibitor (Yeo et al., 2003). The symmetrical KCl conditions were compared between SH and co-treatment with 10 μM YC-1 treated cells. The hypoxic upregulation of TASK-2 current was prevented by co-treatment with 10 μM YC-1 (Fig 15D, n=10).

The upregulation of TASK-2 and subsequent membrane hyperpolarization may augment the electrical driving force for Ca^{2+} influx. To test this inference, Ca^{2+} signals activated by BCR stimulation were compared. Bath application of αIgM raised $[Ca^{2+}]_c$, and the change of $[Ca^{2+}]_c$ ($\Delta R_{340/380}$) was higher in SH cells than control (Figs. 16A, n=10). The augmented Ca^{2+} signal by SH was not observed when the membrane

potential was abolished by high K^+ (145 mM KCl)-induced depolarization (Fig. 16B, n=22), which further proved the role of enhanced electrical driving force for Ca^{2+} influx.

The functional expression of TASK-2 in mouse splenic B cell was reported previously (Nam et al., 2011). Therefore, we tested whether the hypoxic upregulation of TASK-2 is also observed in fresh isolated B cells. The isolated splenic B cells were divided into two groups and incubated in the control or SH condition. In the w-c current was measured between 20 and 28 h after the isolation. Owing to the small size of primary B cells (ca. 0.8 pF of whole cell membrane capacitance), single channel activities of outward K^+ channels could be discriminated in the w-c configuration. The pH-sensitive outward current at 0 mV and the single channel amplitudes of around 1.8 pA at 0 mV were consistent with the properties of TASK-2 channels. The TASK-2 like channels showed increase and decrease of activities (NP_o) by alkaline (pH 8.4) and acidic (pH 6.4) pH_e, respectively (Fig. 17A, B). In control cells, rarely observed the pH_e-sensitive TASK-2-like channels. In SH cells, however, TASK-2-like pH_e-sensitive channels, and their activities (NP_o) were generally higher than the control group (Fig. 17C).

	Bath solution					Pipette solution	
Solute (mM)	NT	NT (pH)	High K^+ (i-o)	High K^+ (w-c)	High K^+- DVF (w-c)	High K^+ (Ca^{2+} free, w-c)	High K^+ (i-o)
NaCl	145	145	(-)	(-)	(-)	5	(-)
KCl	3.6	3.6	145	140	140	140	145
$CaCl_2$	1.3	1.3	(-)	1	(-)	(-)	(-)
$MgCl_2$	1	1	(-)	1	(-)	0.5	(-)
Glucose	5	5	(-)	5	5	(-)	(-)
HEPES[1]	10	5	10	5	10	10	10
MES	(-)	5	(-)	5	(-)	(-)	(-)
EGTA	(-)	(-)	1	(-)	(-)	5	1
MgATP	(-)	(-)	(-)	(-)	1	3	(-)
pH	7.4	6.4~8.4	7.2	6.4~8.4	7.4	7.2	7.4

Table 1 Experimental solutions and their compositions.

All the units are in mM except pH. NaOH or KOH were used to adjust pH values in bath and pipette solutions. HEPES; 4-(2-hydroxyethyl)-1-piperazine ethanesulfonic acid, MES; 2-(N-morpholino) ethanesulfonic acid, EGTA; 2-bis(2-aminophenoxy)ethane-N,N,N′,N′-tetraacetic acid, w-c; whole cell patch clamp, o-o; outside-out patch clamp

Protein (Gene Bank #)	Primer	Size (bp)	Sequence (5' to 3')
Mouse TASK-1	Forward Reverse	237	CGTGTGCACCTTCACCTACC ATGACGGTGATGGCGAAGTA
Mouse TASK-2	Forward Reverse	208	ACTGGAAGGAGGCCAAGAAA ATGGTGGTGATGACTGTGGC
Mouse TASK-3	Forward Reverse	106	CAGACGTGCTGAGGAACACC TAGATGGACTTGCGACGGAG
Mouse TASK-5	Forward Reverse	203	AGAAAGTACCGCTTCTCCGC CCCAGGAGGGCATAGAACAT
Mouse GAPDH	Forward Reverse	275	CCCACTAACATCAAATGGGG CCTTCCACAATGCCAAAGTT
Mouse HIF-1α	Forward Reverse	350	GTCGGACAGCCTCACCAGACAG TCTGCATGCTAAATCGGAGGGT
Mouse 18s rRNA	Forward Reverse	186	CGGCTACCACATCCAAGGAA GCTGGAATTACCGCGGCT

Table 2 Nucleotide sequences of the primers used for RT-PCR

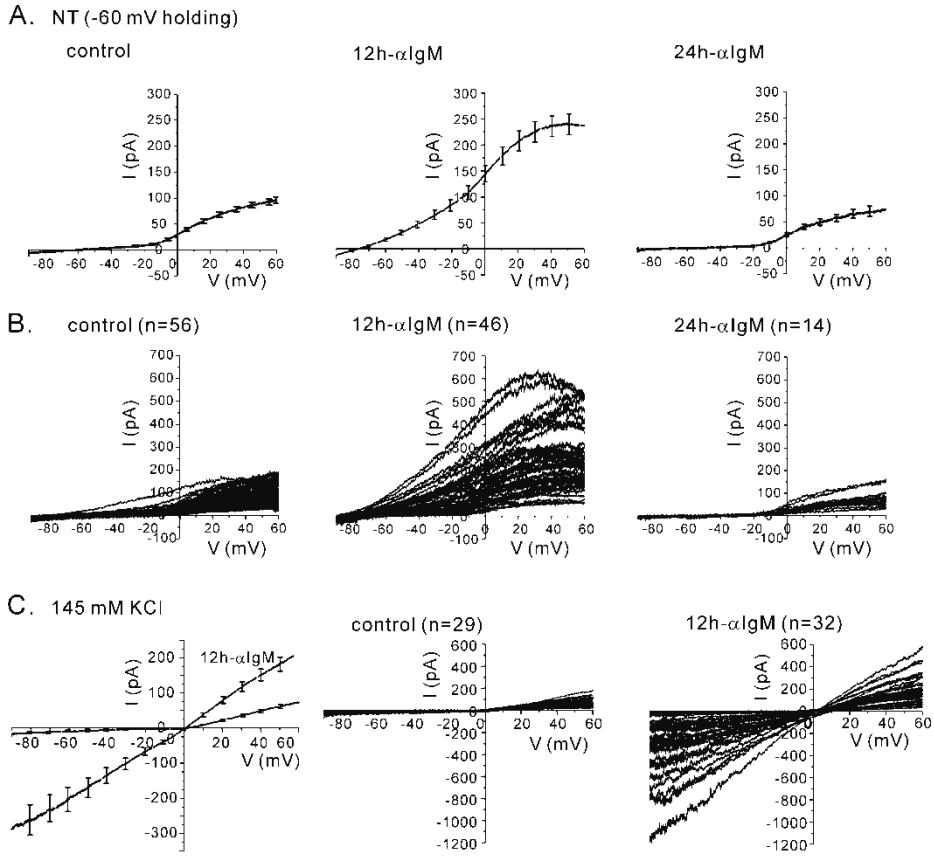

Figure 1. Increase of background type K^+ currents by BCR-ligation in WEHI-231 cells

(A, B) Membrane currents of WEHI-231 cells in the control (left, n=56), 9-15 h after αIgM treatment (middle, 12 h- αIgM, n=46), and 24-30 h after αIgM treatment (right, 24 h- αIgM, n=14) groups were obtained under w-c clamp conditions. The membrane voltage was held at -60 mV and I/V curves were obtained by applying depolarized ramp pulses from -90 to 60 mV. In **A**, I/V curves of each group were averaged and results

are displayed with SEM. In B, superimposed original I/V curves of individual cells obtained under each condition are shown. (C) The increased voltage-independent K^+ conductance in 12 h-αIgM was also confirmed under symmetrical K^+ conditions. Mean membrane currents in the control (n=29) and 12 h-αIgM cells (n=32) are shown in the left panel. Superimposed original I/V curves from individual cells are also shown in the middle (control) and right (12 h-αIgM) panels.

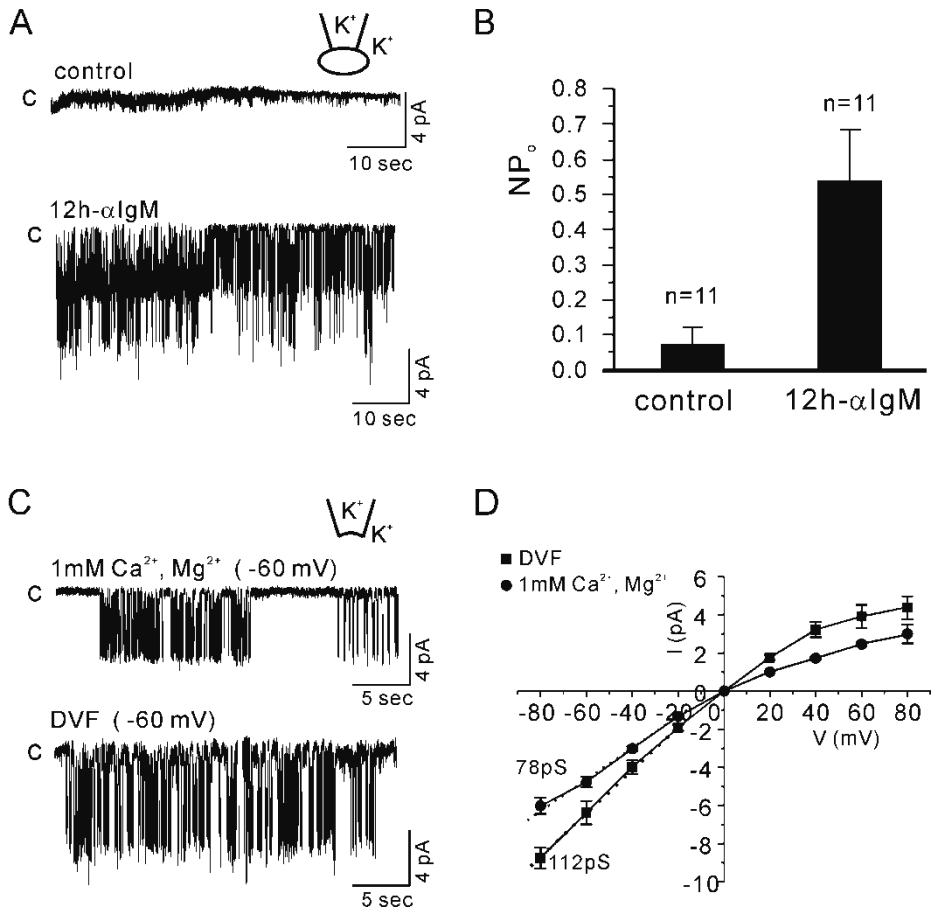

Figure 2. Increased activity of MK_{bg} by BCR-ligation in WEHI-231 cells

(A) Representative single-channel current traces under c-a conditions at 60 mV (pipette voltage, symmetrical KCl solutions) in control and 12 h-αIgM cells. Throughout the figures, the letter 'c' and horizontal arrows indicate the closed and open levels of MK_{bg}, respectively. (B) Summary of the effect of BCR-ligation on MK_{bg} activity recorded in c-a condition. MK_{bg}

activity (np_o) was 7.4-fold higher in 12 h-αIgM cells. **(C)** Representative traces of i-o recording in the absence (DVF) or presence of divalent cations (1 mM Mg^{2+} and Ca^{2+}) in pipette solution. **(D)** Mean values of single channel amplitudes were plotted against clamped voltage. A linear fitting at negative voltage yielded 78 pS and 112 pS with and without divalent cations, respectively.

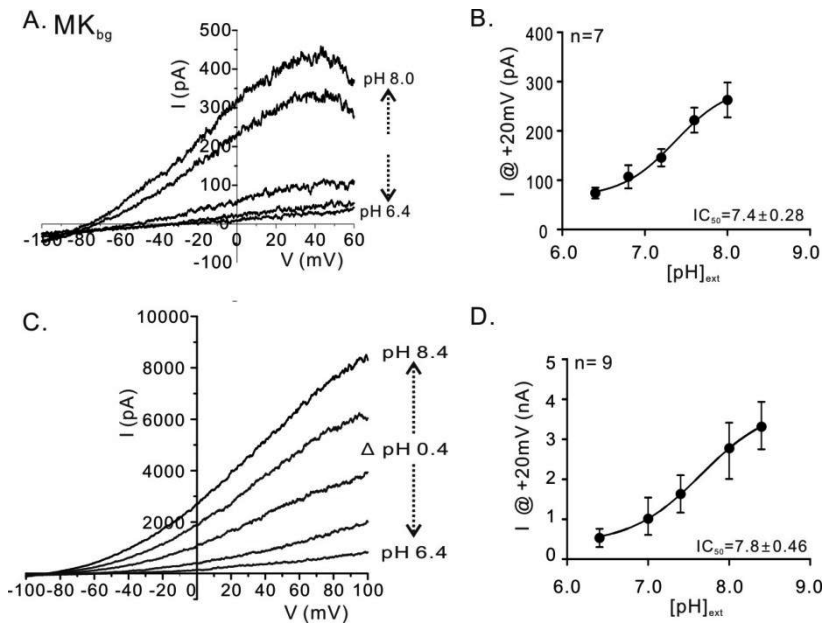

Figure 3. pH_e-sensitivity of MK_{bg} current induced by BCR-ligation

(A) Representative current traces in 12 h-αIgM cells at different pH_e values (8.0, 7.6, 7.2, 6.8 and 6.4, respectively). Cells were held at −10 mV and ramp pulses (from −100 to 80 mV) were applied. (B) Amplitudes of currents at 20 mV were measured for each pH_e and summarized values are plotted (means ± SEM, n=7-9). Fitting the results with a Hill function yielded a half-effective pH_e of 7.4. (C) Representative current traces of mTASK-2 overexpressed HEK293T cells at different pH_e values (8.0, 7.6, 7.2, 6.8, and 6.4, respectively). HEK293T

cells were held at −80 mV between ramp pulses. (D) pH_e-dependence of mTASK-2 overexpressed in HEK293T cells. Mean amplitudes of outward current at 20 mV are plotted with SEMs (n=4-7), and were fitted a Hill function. The half inhibitory pH_e was 7.5, which was similar to that of the 12 h-αIgM induced K^+ current in WEHI231 cells (IC_{50}=7.4).

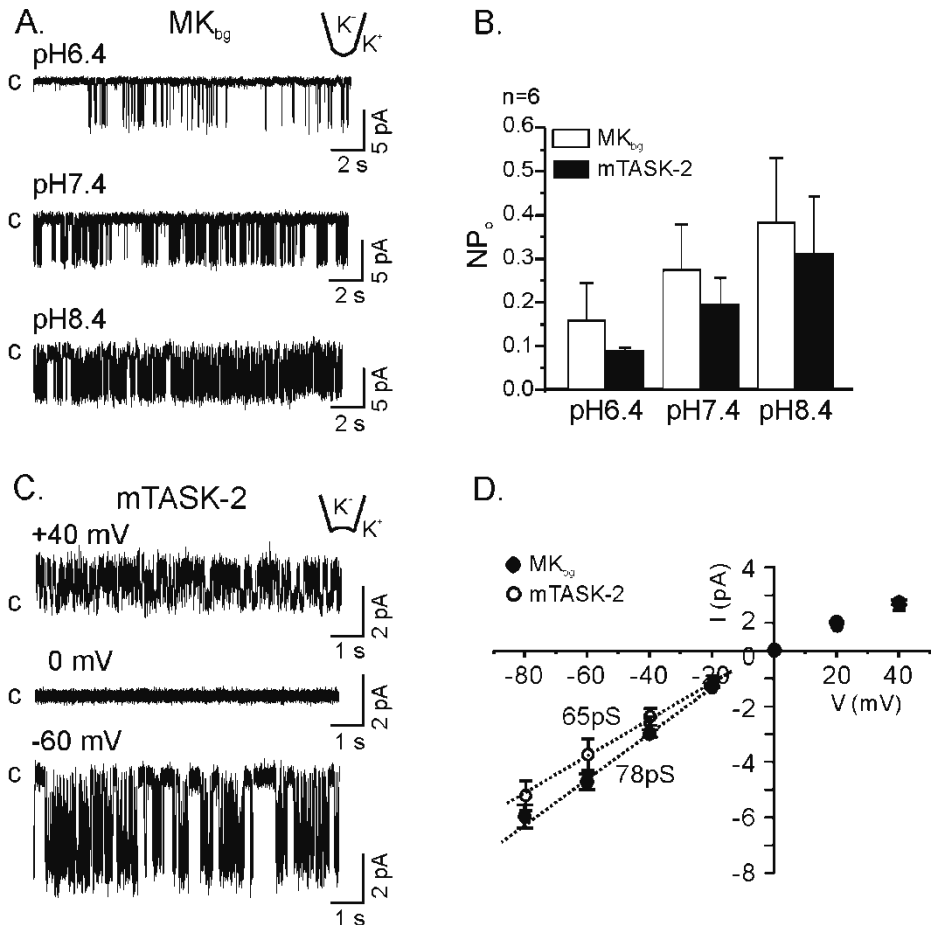

Figure 4. Inhibition of MK_{bg} by acidic pH_e

(A) Representative current traces of o-o patch clamp recordings showing the pH_e-sensitivity of MK_{bg} in 12 h-αIgM WEHI-231 cell. (B) Comparison of the summarized pH_e-sensitivities of MK_{bg} and mTASK-2. In each patch, the np_o of MK_{bg} and TASK-2 at pH_e 6.4, 7.4, and 8.4 were measured, and averaged values are displayed (n=5). (C) Representative current traces of mTASK-2 at different holding voltages (40, 0,

and −60 mV). (D) I/V curves of unitary currents for MK_{bg} and mTASK−2 recorded under i−o configuration with symmetrical $[K^+]$ (145 mM). Each represents mean ± SEM. A linear fitting at negative voltages yielded 78 pS for MK_{bg} and 65 pS for mouse TASK−2. The result for MK_{bg} is duplicated from Fig. 2D.

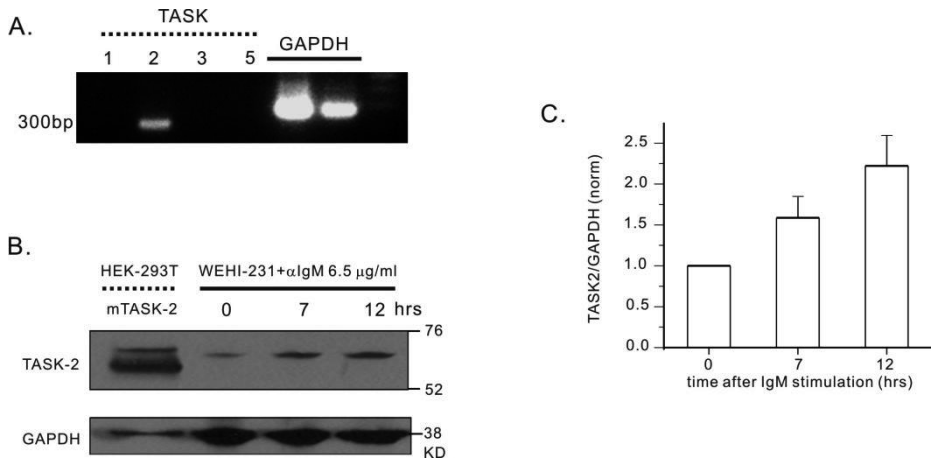

Figure 5. Molecular identification of MK_{bg} as TASK-2

(A) RT-PCR detection of TASK-2 mRNA in WEHI-231 cells. Agarose gel electrophoresis of PCR products generated using specific primers for mouse TASK-1, TASK-2, TASK-3 and TASK-5. As a control, GAPDH mRNA was also detected using specific primers. (B) Immunoblot assay for mTASK-2 in WEHI-231 cells. Cells were incubated in culture medium containing αIgM (6.5 μg/ml) for 0, 7 or 12 h. Protein samples were also obtained from mTASK-2 overexpressing HEK293T cells as a positive control for the antibody. (C) Summary of the immunoblot assay (n=4). Increased density ratios (TASK-2/GAPDH) indicate the up-regulation of mTASK-2 in WEHI-231 cells by BCR-ligation.

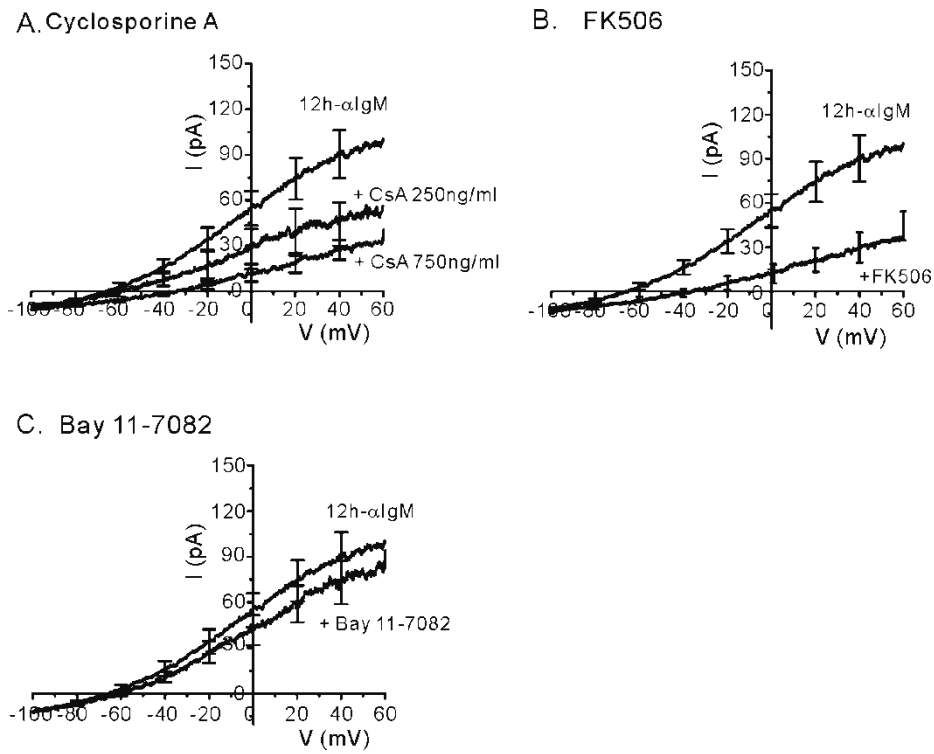

Figure 6. Calcineurin−dependent for TASK−2 up−regulation in WEHI−231 cells

(A−C) Cells were held at −10 mV to inactivate K_v current, and reverse ramp pulses (from 60 to −100 mV) were applied. Cells were stimulated with αIgM (6.5 μg/ml, 12 h) alone or co−treated with cyclosporine A (CsA, n=8 for 250 ng/ml, n=13 for 750 ng/ml), FK506 (n=16), or with Bay 11−7082 (10 μM, n=11). The increase of outward current by 12 h−αIgM was prevented by co− cyclosporine A (A) or FK506 (B) Bay 11−7082 did not affect the increase of outward current (C).

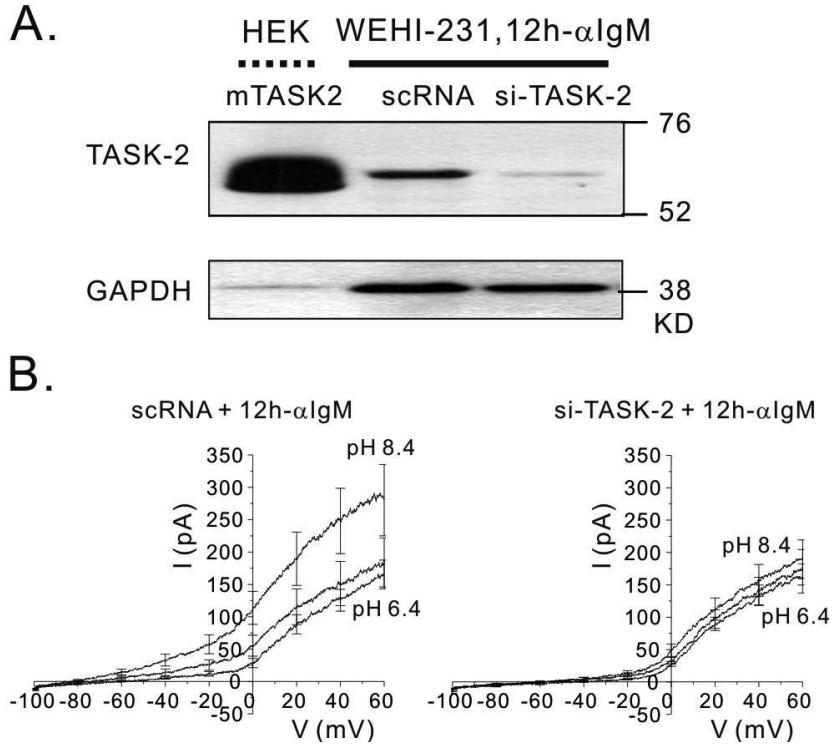

Figure 7. Effects of siTASK-2 in WEHI-231

(A) Effects of siTASK-2 transfection on MK_{bg} by BCR-ligation. Either scRNA (200 nM) or siTASK-2 was transfected. Then, WEHI-231 was stimulated with αIgM (6.5 μg/ml, 12 h), and protein samples were collected. Immunoblot assays showed reduced TASK-2 in the siTASK-2 transfected WEHI-231 cells. As a positive control, mTASK-2 overexpressed HEK293T cells were also prepared for the assay (left most lane, HEK). (B) The pH_e-sensitive K_{bg} current was not induced by BCR-ligation in siTASK-2 transfected WEHI-231 cells.

Depolarizing ramp pulses (from −100 to 60 mV) were applied to obtain I/V curves, and summarized results (means ± SEM.) are shown for scRNA and siTASK−2 transfected WEHI−231 cells (n=14, respectively).

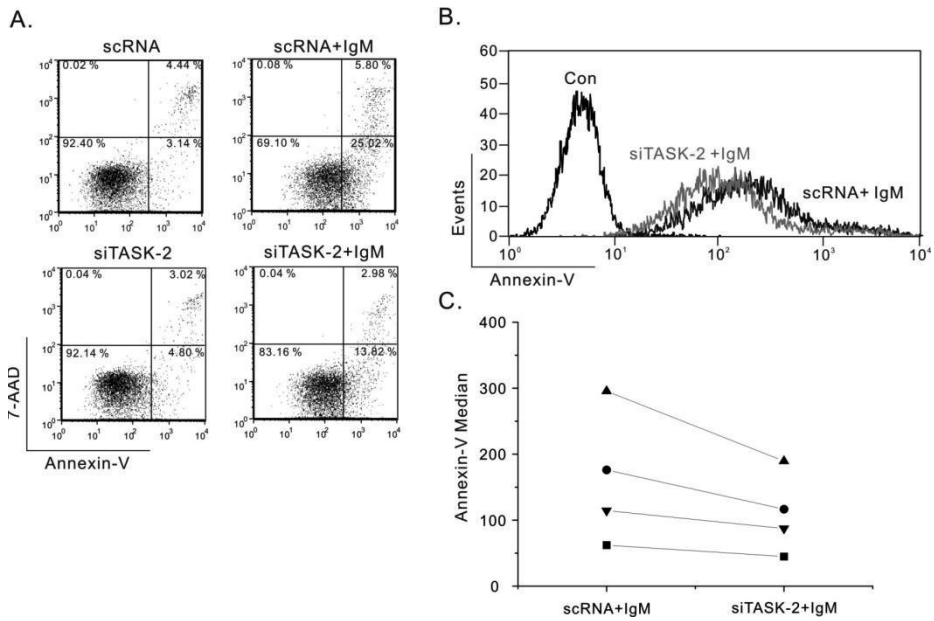

Figure 8. Roles of TASK-2 causing apoptosis in WEHI-231

Annxin-V a 7-AAD double staining assay. (A) WEHI-231 cells were divided into four treatment groups; the scRNA-transfected control (left upper), the scRNA-transfected 48 h-αIgM (right upper), the siTASK-2 transfected control (left lower), and the siTASK-2 transfected 48 h αIgM (right lower) group. Cells were stained with Annexin-V-FITC (horizontal axis) and 7AAD-PE (vertical axis) for flow cytometry. The proportions (%) of Annexin-V(+) or 7-AAD(+) cells are indicated in the figure. (B) Representative histograms of the scRNA (black) or siTASK-2 (gray) transfected cells. (C)

The median of annexin-V positive cell in scRNA or siTASK-2 under 48 h α-IgM group (n=4).

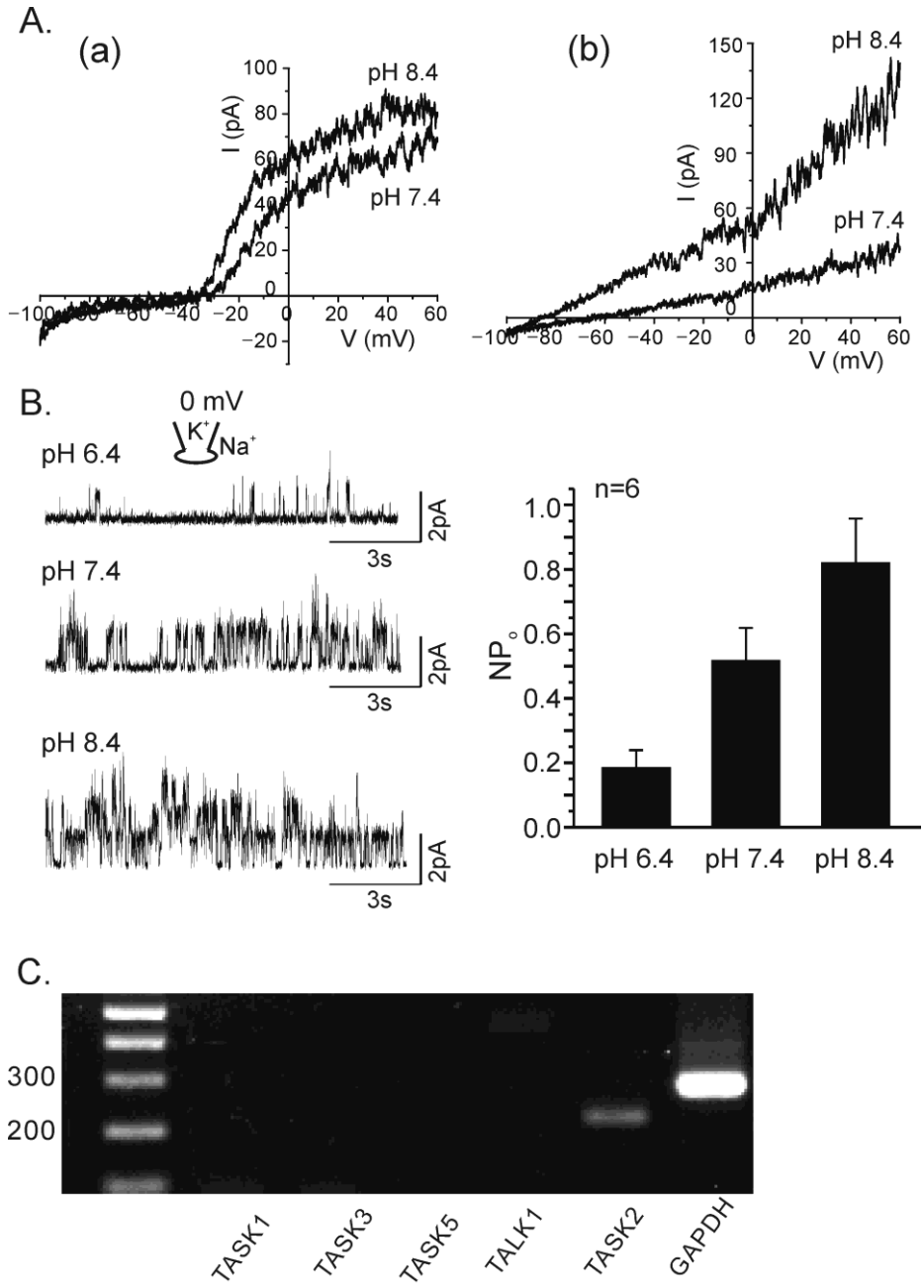

Figure 9. Expression of TASK-2 in primary B cells

(A) In w-c configuration, mouse splenic B cells were held at -60 mV, and ramp-like pulses (from -100 to 60 mV) were

applied to obtain brief I/V curves. I/V curve in the left panel (a) shows a K_v predominant case where alkaline pH_e (8.4) only slightly increased the outward current. The right panel (b) demonstrates a representative case of alkaline pH_e-activated background K^+ current. **(B)** Left; representative traces of pH_e-sensitive K^+ channels in the o-o configuration of a mouse splenic B cell. NT bath solution was used and the membrane voltage was held at 0 mV to selectively record K^+ channel activity. pH_e values of bath solutions are indicated above each trace. Right; summary of pH_e-dependent activity (np_o) of the TASK-2-like channels. In each patch, np_o at pH_e 6.4, 7.4, and 8.4 were measured for 60 s, respectively, and averaged (n=6). **(C)** RT-PCR analysis of mouse splenic B cells for TASK-1, 3, 5, TALK-2 and TASK-2. Positive signal of TASK-2 mRNA (208 bp) shown.

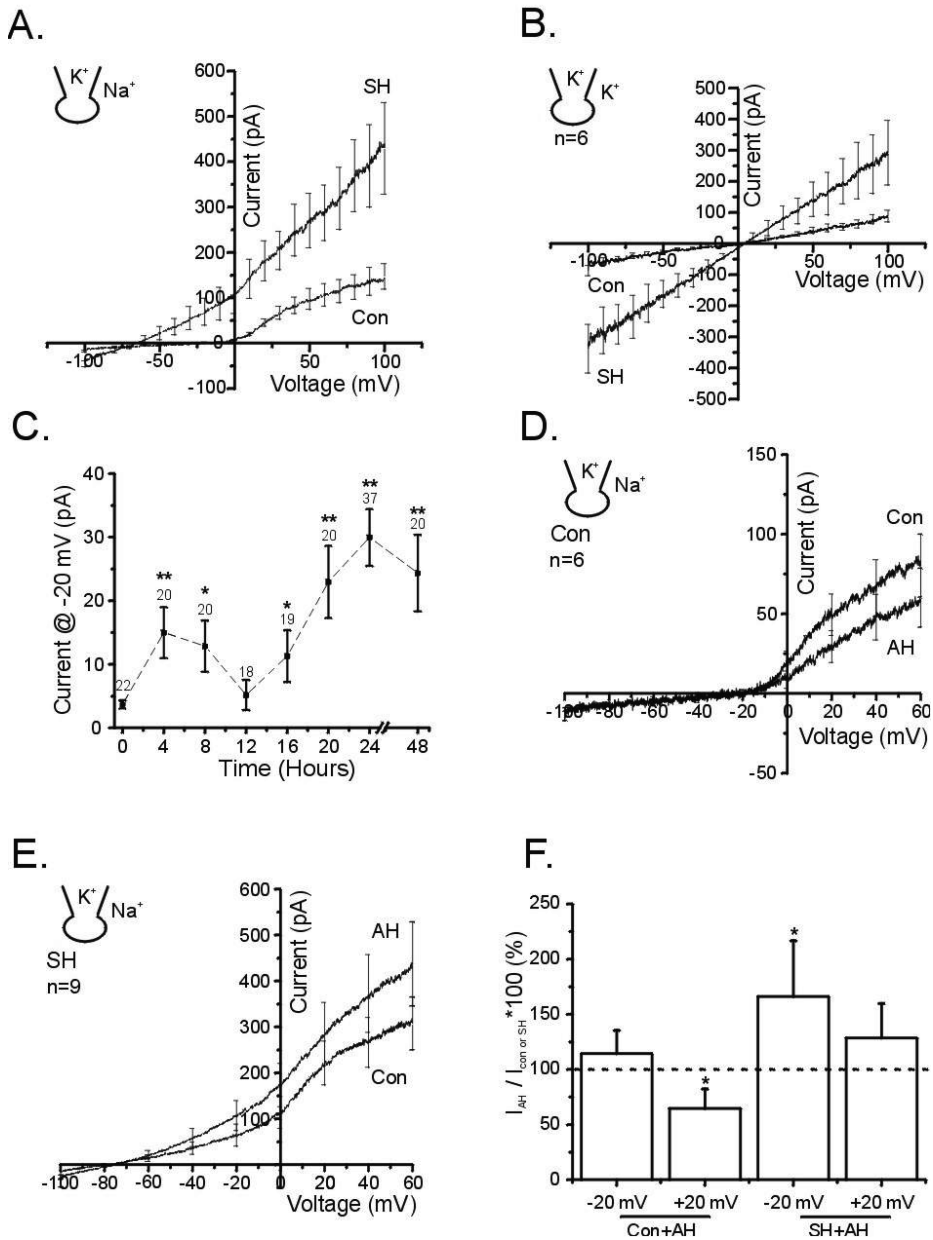

Figure 10. Sustained hypoxia induces background K^+ current in B cells

(A) Comparison of membrane currents of WEHI-231 between control and SH cells. In the w-c clamp conditions, I/V curves

were obtained by ramp-like pulses (from −100 to 100mV, holding voltage −60 mV). Note the increase of K_{bg} current in SH cells. **(B)** Under symmetric K^+ conditions, the induction of K_{bg} conductance was also confirmed as inward current in the SH cells. **(C)** Time-dependent induction of K_{bg} current by hypoxic culture conditions. Mean amplitudes of outward current at −20 mV are plotted according to the duration (hours) of hypoxia. Numbers of tested cells are indicated above each point (mean ± SEM) (**$P < 0.01$, *$P < 0.05$). **(D)** Inhibitory effect of AH on K_v currents in control WEHI-231 cells. **(E)** Augmentation of K_{bg} current by AH in SH cells. Throughout the figures, I/V curves obtained in each group were averaged and plotted with vertical bars indicating SEM. **(F)** The normalized current amplitudes at −20 mV and +20 mV are shown in the bar graph (mean ± SEM) (*$P < 0.05$).

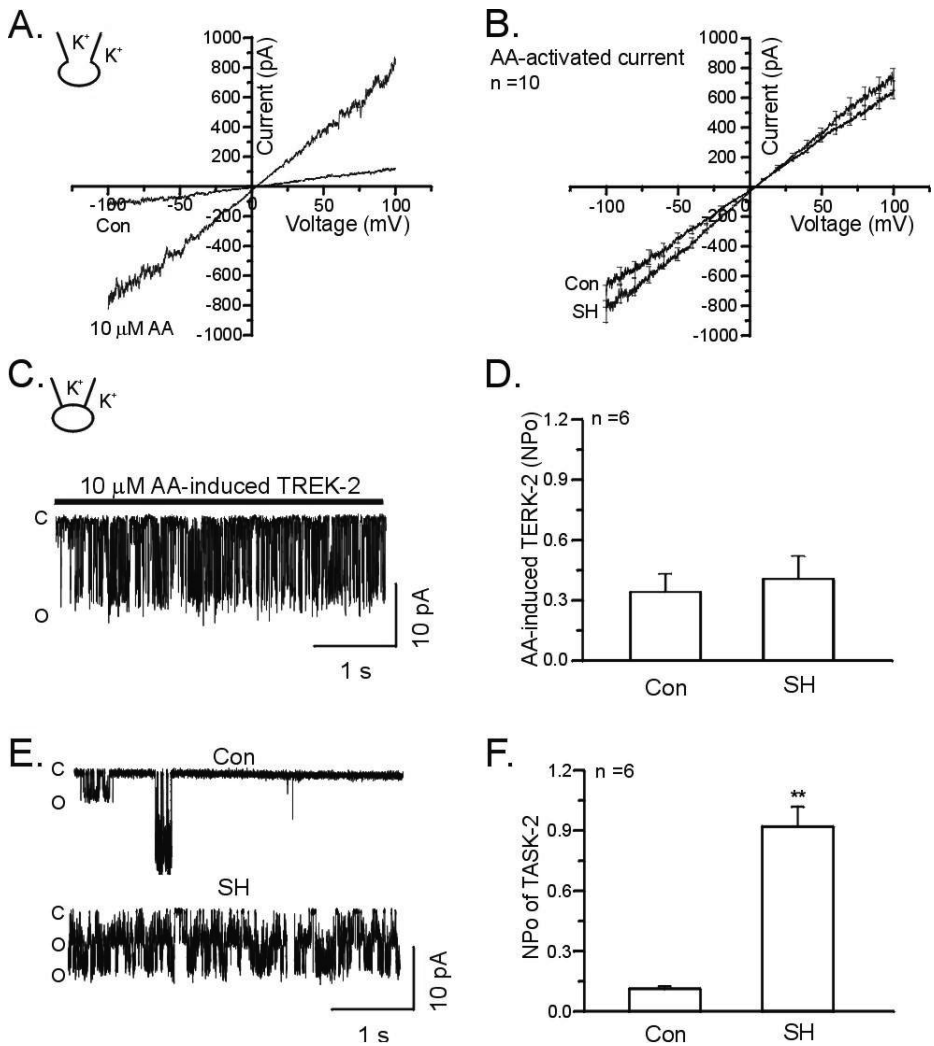

Figure 11. Induction of TASK-2 like K^+ channels in WEHI-231 cells undergoing SH

(A) Activation of TREK-2 K^+ current by arachidonic acid (AA, 10 μM) in WEHI-231 cell. To reveal the voltage-independent K^+ current activity, I/V curves of K^+ conductance were obtained under symmetrical KCl conditions. (B) AA-induced current was obtained by digital subtraction of initial current from the current with 10 μM AA, and the averaged I/V

curves are compared between control and SH-cells (n=10). **(C)** In c-a configuration under symmetric KCl conditions, application of 10 μM AA activated inward K^+ current with relatively large single channel conductance (17 pA at -60 mV), which was consistent with TREK-2. **(D)** The activity of AA-induced TREK-2 (NPo) was not different between control and SH-cells (n=6). **(E)** TASK-2 like K+ channel current with 5.5 pA of single channel current (at -60 mV) was rarely observed in control cells (upper) whereas frequently observed in SH-cells (lower). **(F)** The averaged values of TASK-2 like channel activity (NPo) were definitely higher in SH-cells (n=6) (**$P < 0.01$).

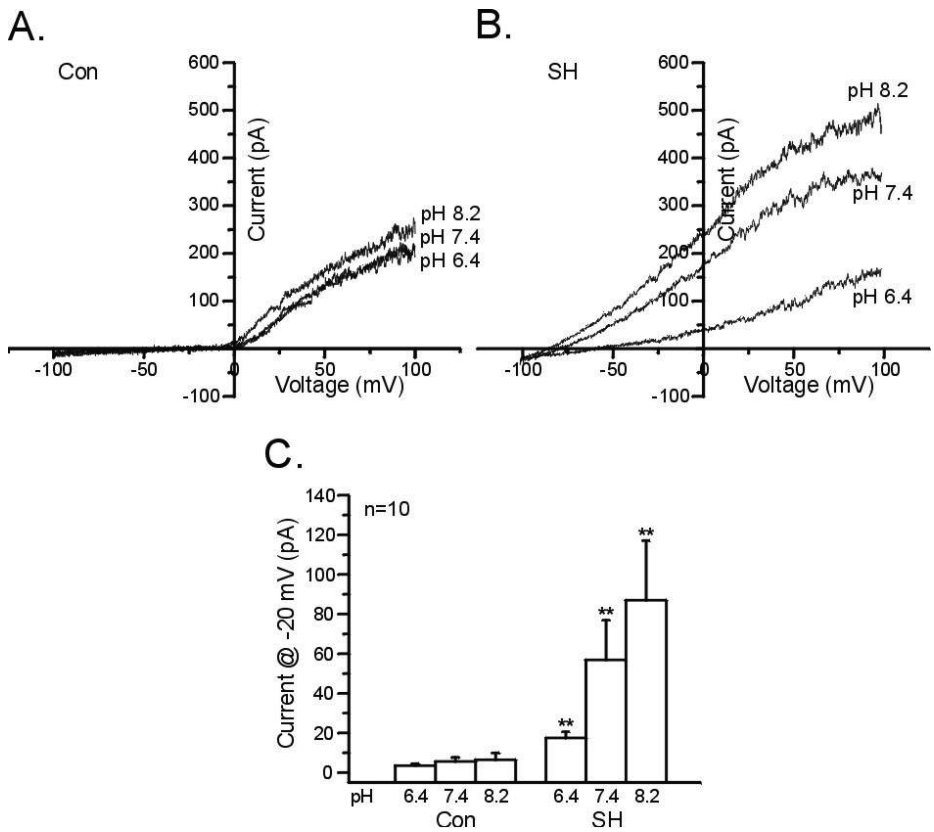

Figure 12. pH_e−dependence of SH induced K_{bg} current

Representative current traces of control (A) and SH−cells (B) at differential pH_e (6.4, 7.4 and 8.2). (B) The K_{bg} current of SH−cell was increased and decreased by pH 8.2 and 6.4, respectively. (C) Summary of current amplitudes at −20 mV for each pH_e (mean ± SEM, n=10) ($^{**}P < 0.01$).

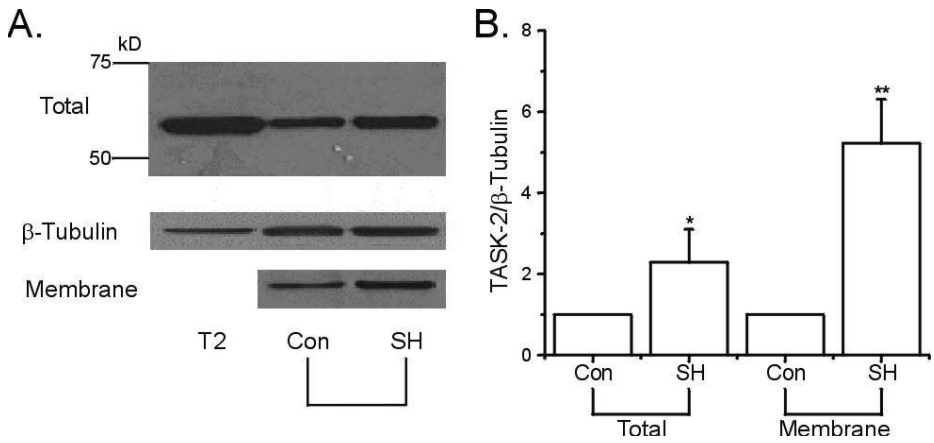

Figure 13. SH increased the protein expression of TASK-2 in B cells

Immunoblot assay for mTASK-2 in WEHI-231 cells. Cells were incubated in control and SH condition. Protein samples also obtained from mTASK-2 overexpressed in HEK293T cells as a positive control (T2) for the antibody. (A) Total and membrane fraction of mTASK-2 protein expression were significantly increased in B cells. (B) Summary of the immunoblot assay. Increased density ratios (TASK-2/β-tubulin) normalized to the initial level indicates the up-regulation of mTASK-2 in WEHI-231 cells by hypoxia. (mean ± SEM, n=4) (**$P < 0.01$, *$P < 0.05$).

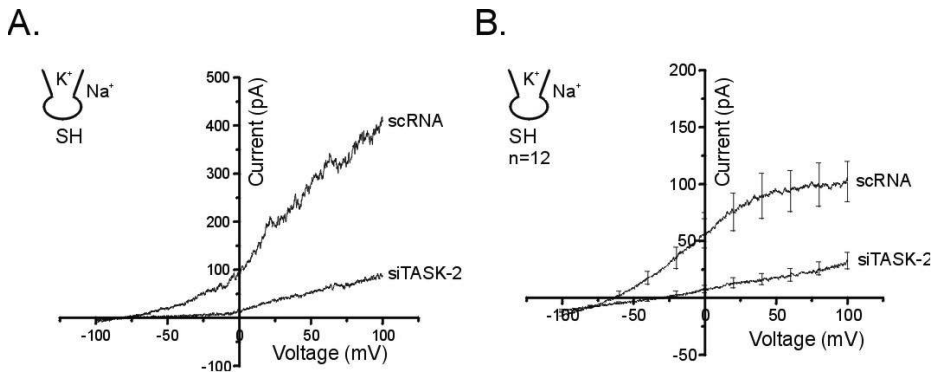

Figure 14. Inhibition of SH induced K_{bg} current by siTASK-2 transfection

(A) Representative I/V curves obtained by depolarizing ramp pulse from −60 mV holding voltage in scRNA and siTASK-2 transfected SH cells. (B) To exclude K_v conductance, membrane voltage was held at depolarized level (20 mV), and reverse ramp pulses (from 100 to −100 mV) were applied. Summarized results (means ± SEM) are shown for scRNA and siTASK-2 transfected WEHI-231 cells (n=12, respectively).

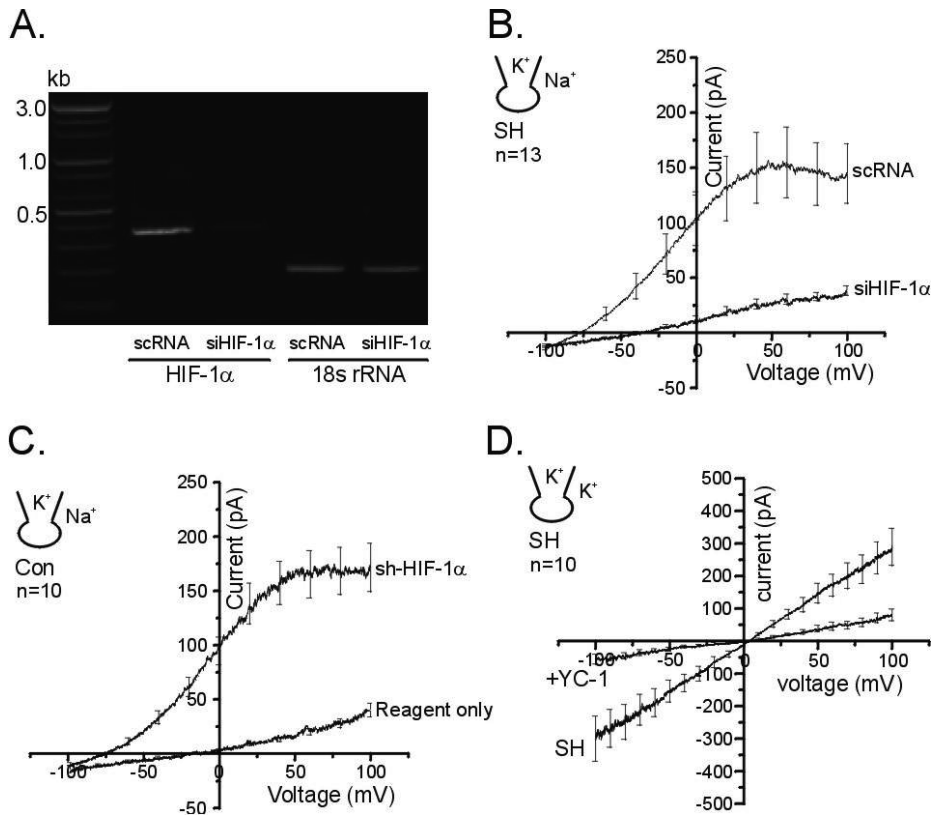

Figure 15. HIF−1α mediates SH activation of TASK−2 in B cells

(A) RT−PCR analysis for HIF−1α in scRNA and siHIF−1α transfected SH−cells, showing abolished HIF−1α mRNA by siHIF−1α. (B) Comparison of TASK−2 current between scRNA and siHIF−1α transfected SH cells. I/V curves were obtained by repolarizing ramp pulses (holding voltage, 20 mV). TASK−2 current was largely abolished in the siHIF−1α transfected SH−cells. (C) Upregulation of TASK−2 current by overexpression of O_2−resistant sh−HIF−1α (0.5 μM) in WEHI−231 cells under control condition (n=10). (D) Inhibitory effect of YC−1, a HIF−1 inhibitor on TASK−2 induced by SH. Summary of I/V curves

obtained in symmetrical KCl conditions (n=10, holding voltage, 0 mV).

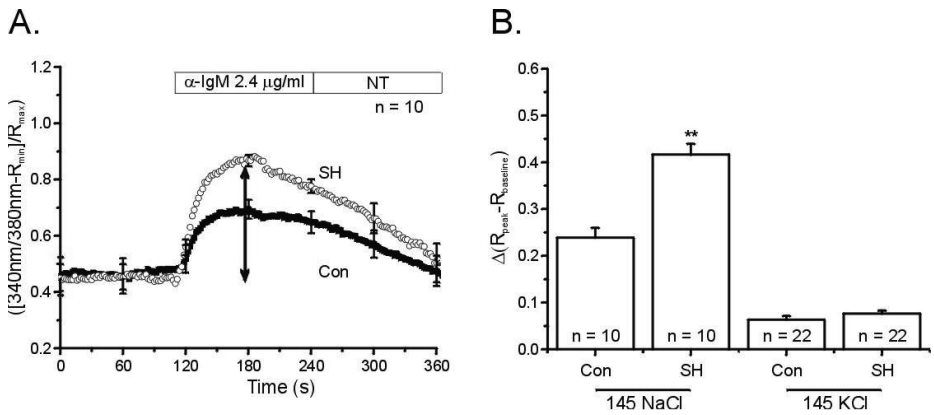

Figure 16. Augmented Ca^{2+} signal by BCR stimulation in SH cells

(A) Normalized fura-2 fluorescence ratio of single WEHI-231 cell, an indicator of $[Ca^{2+}]_c$, was increased by BCR stimulation with αIgM (2.4 μg/ml). Averaged results from 10 cells for each group, control and SH cells, displayed higher amplitudes of $[Ca^{2+}]_c$ changes. (B) Peak changes in $[Ca^{2+}]_c$ ($\Delta R_{340/380}$) were summarized for each group (control vs. SH) in NT and high KCl solutions, respectively. It is notable that the $\Delta R_{340/380}$ was attenuated in KCl solution with no difference between control and SH cells (**$P < 0.01$).

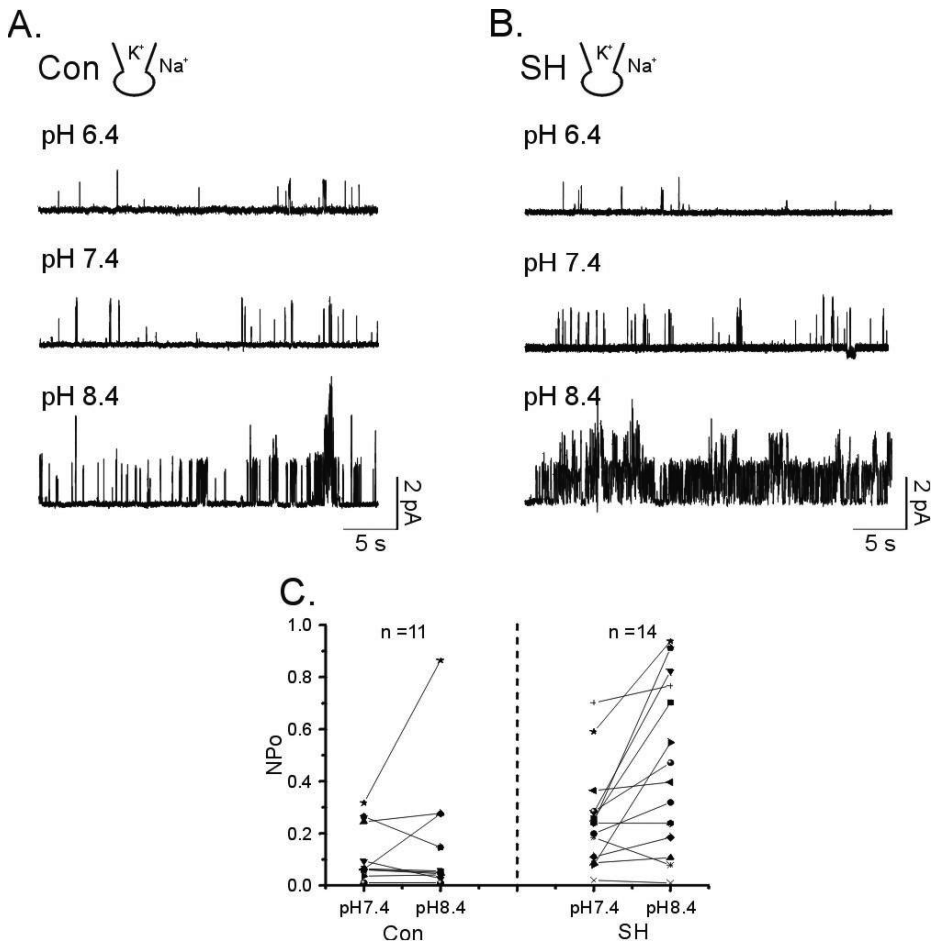

Figure 17. Higher activity of TASK-2 channels in primary splenic B cells undergoing SH

(A, B) Representative traces of pH_e sensitive K^+ channels in mouse splenic B cells after control incubation (A) and SH (B). NT bath and High K^+ pipette solution were used, and the membrane voltage was held at 0 mV to selectively record K^+ channel activity in c-a configuration. pH_e values of bath solutions are indicated above each trace. (C) The summary of

pH_e dependent activity (NPo) of the TASK-2-like channels. In each patch, NPo at pH_e 7.4, and 8.4 was measured during 40 s, respectively. In control cells, rarely observed the pH_e-sensitive TASK-2-like channels. In SH cells, however, TASK-2-like pH_e-sensitive channels, and their activities (NP_o) were generally higher than the control group.

DISCUSSION

In this study, I present that the K_{bg} in mouse B lymphocytes, is TASK-2 (judging by biophysical property, conductance of 78 pS and by pH sensitivity). The expression of TASK-2 in WEHI-231 cells is markedly upregulated by BCR-ligation, which may be associated with the apoptosis of B lymphocytes. Similarly, SH condition significantly increased TASK-2 channel in WEHI-231 cells via HIF-1α dependent mechanism. Furthermore, increased TASK-2 activity was associated with augmented Ca^{2+} responses (Hyperpolarization) to BCR-ligation, which is critical for B cell activation.

K2P channels in T, B lymphocytes

The functional roles of K2P channels in lymphocytes have received attention and the studies undertaken so far have been performed on T cells (Meuth et al., 2008; Pottosin et al., 2008). Immunological studies on T cells have suggested that TASK-1 and TASK-2 have aggravating roles in autoimmune encephalomyelitis and multiple sclerosis, respectively (Bittner et al., 2010). In these studies, however, there was no direct electrophysiological evidence indicating the TASK or TALK

family of K2P channels. Accordingly, I describe for the first time, electrophysiological properties of TASK-2 channels in B lymphocytes.

The unitary conductance of TASK-2 is greater than that of any other member of the TASK and TALK subfamilies of K2P channels. Although the conductance of TASK-2 like channel in the B lymphocytes is slightly greater than that of cloned mTASK-2 (Fig. 4D), it falls within the range of those previously reported for TASK-2 (Kim et al., 2005; Lotshaw et al., 2007). The difference in slope conductance might be due to dissimilar expression background (WEHI-231 vs. HEK293T).

The RT-PCR analysis of WEHI-231 and primary B cells demonstrated that the transcripts for TASK-2 are predominantly expressed among the pH_e-sensitive K2P channels (Fig. 3 and Fig. 9).

TASK-2 channel in other organs

TASK-2 was initially found in human kidney, and tissue distribution studies show expressions of TASK-2 in epithelium from a number of organs such as, pancreas, placenta, lung, intestine, and kidney (Reyes et al., 1998).

Immunohistochemistry results also confirm that TASK-2 is expressed in rat hippocampus (Gabriel et al., 2004). In addtion, functionally active native TASK-2 was reported in cerebellar granule cells (Cotton et al., 2004). As shown in this study, TASK-2 is sensitive to pH_e and the half-effective pH_e of cloned TASK-2 is known to be close to physiological pH (Fig. 3C) (Lotshaw et al., 2007).

In kidney, TASK-2 in proximal tubules is important for $NaHCO_3$ absorption, as suggested from the phenotypes of metabolic acidosis and hypotension in TASK-2 deficient mice (Warth et al., 2004). In addition, TASK-2 has been linked to the control of excitability in intestinal smooth muscle (Cho et al., 2005) and cerebellar granule cells (Cotton et al., 2004). Intriguingly, TASK-2 has also been suggested to participate in the regulation of cell volume (Niemeyer et al., 2001; Kirkegaard et al., 2010), and in the apoptotic volume decrease (AVD) of proximal tubular epithelium (Barriere et al., 2003; L' Hoste et al., 2007). My results suggest that the TASK-2 upregulation by BCR-ligation might be associated with apoptosis of B lymphocytes (Fig. 1, 8).

Physiological implication of the TASK-2 expression in B lymphocytes

Both RT-PCR analysis and immunoblot studies indicate the expression of TASK-2 in splenic B cells (Fig. 5, 9).

Different from the mechano- and arachidonic acid-activated TREK/TRAAK subfamily of K2P channels, the members of the TASK and TALK subfamilies display genuine 'background' activity. In this respect, the significant upregulation of TASK-2 by BCR-ligation or prolonged hypoxia suggests that a hyperpolarization of lymphocytes would have been induced.

In B lymphocytes as well as other immune cells, role of ion channels is usually investigated with respect to Ca^{2+} signals, i.e. Ca^{2+} influx pathways such as calcium-release activated Ca^{2+} (CRAC) channel or transient receptor potential (TRP) family of nonselective cation channels (Liu et al., 2005; Chung et al., 2007). BCR-ligation triggers complex cascades of signalling pathways, which lead to an increase in the $[Ca^{2+}]_c$ via PLCγ2/$InsP_3$ pathway and CRAC/TRP channels. $[Ca^{2+}]_c$ elevation triggers the activation of calcineurin (a protein phosphatase), which can activate target molecules, such as, caspase-2 and NFAT (Eeva et al., 2004). The upregulation of

TASK-2 appears to be tightly associated with calcineurin-dependent signalling pathways (Fig. 6) that link to NFAT-dependent transcriptional regulations during the immunological activation of B lymphocytes (Kurosaki et al., 2002; Scharenberg et al., 2007). Previous studies suggested that the upregulation of TASK- or TRESK channels in T cells is associated with the effecter functions of these cells (Meuth et al., 2008; Bittner et al., 2009). To support the Ca^{2+} influx, hyperpolarized membrane potential is required, and in this respect, the expression and upregulation of TASK-2 would augment the Ca^{2+} signaling (Fig. 16).

Role of TASK-2 in the apoptosis of B lymphocytes

WEHI-231 is widely used as a model of B lymphocytes that show apoptosis under strong BCR stimulation. The present study showed robust upregulation of TASK-2 by BCR ligation. Excessive K^+ efflux might contribute to apoptosis by two mechanisms; 1) osmotic water loss leads to AVD (Trimarchi et al., 2002), and 2) by regulating apoptotic enzymes, such as, nuclease and caspase (Bortner et al., 2007; Lang et al., 2007).

The present study suggests that TASK-2 might participate

in the WEHI-231 apoptosis, because the genetic downregulation of TASK-2 attenuated the cell death induced by BCR-ligation (Fig. 8). The relatively weak inhibitory effect of siTASK-2 on apoptosis might be due to inefficient transfection of siRNA into the floating WEHI-231 cells. Another possible explanation for the limited effect of siTASK-2 is that TREK-2 might also provide the K^+ efflux pathway in BCR stimulated WEHI-231 cells. Unfortunately, the lack of specific blockers for the members of K2P limited our ability to test this hypothesis pharmacologically.

The involvements of K2P channels in apoptosis has been also suggested for other members, such as, TASK-1 and -3 (Patel AJ et al., 2004) and TALK (Duprat et al., 2007). The TASK/TALK subfamily of K2P channels are characterized by a typical leak or background activity, and are open at rest. In contrast, a variety of physicochemical stimuli are required to cause TREK/TRAAK channels to open (Kim et al., 2005; Bayliss et al., 2008). In this respect, TASK/TALK channels are likely to provide a more continuous K^+ efflux than other types of AVD-associated K^+ channels.

Despite the observed effects of siTASK-2 on the apoptosis

of WEHI-231, the actual role of TASK-2 is open to question, because increased background K^+ conductance was found to reverse spontaneously on the day after BCR-ligation. Considering this relatively temporary upregulation, the role of TASK-2 activity in putative AVD is likely to be short-lived, and contributions from other K^+ channels are probably necessary. For example, the cellular microenvironment might provide the conditions (e.g. intracellular acidosis, ROS, and AA) requested to activate TREK channels. Taken together, TREK-2 and TASK-2 might concertedly contribute to AVD of the B lymphocytes *in vivo*.

Putative roles of TASK-2 in hypoxic microenvironments

B lymphocytes are located in lymph nodes and spleen, where oxygen pressure is low (1-5%, depending on the distance to the perfusion vasculature). Such a hypoxic microenvironment *in vivo* ($PhyO_2$) can be graded from hypoxic to anoxic sites such as poorly perfused atherosclerotic regions (Sluimer et al., 2008). Despite this physiological hypoxia is well acknowledged, most biological experiments and cell culture processes are performed at atmospheric P_{O2} ($AtmO_2$, 20-21%).

So far, studies relevant to hypoxic modulation of ion channels in the immune system have been limited to T cells where both AH and SH inhibit $K_v1.3$ channels (Conforti et al., 2003; Szigligeti et al., 2006). The inhibition of K_v current by AH was also observed in this study using B cells (Fig. 10D). The novel finding is that SH upregulates TASK-2, a member of the pH sensitive K2P (KCNK) channel family. It should be noted that the upregulated TASK-2 current in SH cells was further increased by AH (Fig. 10E). Therefore, the hyperpolarizing effect of the upregulated TASK-2 would be valid in the hypoxic/anoxic environments *in vivo*. Among the two types of K2P channels expressed in mouse B cells (Zheng et al., 2009; Nam et al., 2011), total activity of TREK-2 was not altered by SH (Fig. 11D). Ischemic/hypoxic conditions activate phospholipase A_2 (PLA_2) that are responsible for AA production (Lambert et al., 2006), which might potentiate the TREK-2 activity *in vivo* hypoxia. However, another confounding factor for TREK-2 is their putative O_2 sensitivity. Previous studies claimed that hypoxia directly inhibits TREK-1 (Miller et al., 2003), which has high homology with TREK-2. In this respect, the contribution of TREK-2 to the ion channel

mediated immunomodulation under hypoxic/ischemic conditions requires further investigation.

Hypoxic regulation of ion channels can be categorized into an acute response and chronic, sustained up- or down-regulation. The acute inhibitions of K^+ channel have been described in various chemoreceptor cells where subsequent membrane depolarization activates voltage-gated L-type Ca^{2+} channels. In carotid body glomus cells, inhibitions of K_v, ether-a-go-go (hERG), Ca^{2+} activated K^+ (MaxiK) and TASK-1/3 K^+ channels were reported (Buckler et al., 1997; Overholt et al., 2000; Peers et al., 1999; Donnelly et al., 2011). In pulmonary artery smooth muscle cells, the hypoxic inhibitions of Kv and TASK-1 like K^+ channels have been also well described and suggested as the key mechanisms for hypoxic pulmonary vasoconstriction and hypoxic arterial remodeling (Archer et al., 2004). In this respect, the upregulation by SH and the facilitation by AH are relatively unique properties of TASK-2 (Fig. 10).

Recently, TASK-2 was suggested to play a role in the O_2 sensitivity of central respiratory center. TASK-$2^{-/-}$ mice showed disturbed chemosensory function to P_{CO2} changes and

compromised adaptation to chronic hypoxia. In this study, the electrical activity of respiratory center region in the brainstem was suppressed by hypoxia, which was not observed in the TASK-$2^{-/-}$ mice. The authors suggested that the putative ROS generated during the acute hypoxia would have activated TASK-2 channels (Gurney et al., 2010). Interestingly, our study also demonstrated an increase of TASK-2 current by AH in SH WEHI-231 cells (Fig. 10F). The precise cellular mechanisms of TASK-2 facilitation by AH in B lymphocytes require rigorous investigation in future.

In T cells, SH induce functional downregulation of $K_v1.3$ by inhibiting forward vesicular trafficking process (Chimote et al,. 2012). In contrast, the increased current density of TASK-2 in the SH B cells was associated with the increased amount of total and surface protein expression (Fig. 13).

Involvement of HIF-1 signaling in the hypoxic up-regulation of TASK-2

In this study, both pharmacololgical (YC-1) and genetic (siHIF-1α) inhibitions of HIF-1 α activity indicated that the hypoxic up-regulation of TASK-2 is mediated by translational

regulation from HIF-1α (Fig. 15B, D). In addition, the increase of background K^+ current under control conditions by sh-HIF-1α overexpression strongly suggest that HIF-1-depenent translational regulation is sufficient for the induction of TASK-2 in B cells (Fig. 15C). Consistently potential HIF-1 binding region has consistently been identified in the promoter regions of the TASK-2 gene (Brazier et al., 2005). HIF-1 mediated cellular responses cover a wide variety of adaptive and pathological changes during hypoxia (Palazon et al., 2012). Abnormal peritoneal B-1 like lymphocytes are frequently observed in HIF-1α KO mice, and such phenomenon are postulated to be associated with autoimmunity (Kojima et al., 2002). The HIF-1α mediated upregulation of TASK-2 in B cells might also play a role in the systemic adaptation in terms of humoral immune responses and B cell differentiation.

The present study demonstrates that hypoxia is strongly associated with TASK-2 upregulation and membrane hyperpolarization. In fact, WEHI-231 cells exposed to SH showed augmented $[Ca^{2+}]_c$ elevation by BCR-ligation. Since the chemical depolarization (high K^+ conditions) abolished the difference between control and SH cells, it was suggested that

the hyperpolarization inferred from TASK-2 up-regulation was responsible for the augmented Ca^{2+} signal (Fig. 16), which might implicate positive influence on B cell responses.

Interestingly, according to literature, the stimulated primary T cells proliferate better at $AtmO_2$ (McNamee et al., 2013; Atkuri et al., 2005; Loeffler et al., 1992) whereas B cells showed higher proliferation and antibody production at $PhysO_2$ (Singh et al., 1977). The SH-induced changes of K^+ conductance appear to be opposite between T and B cells. A series of studies consistently demonstrated that hypoxia produces both acute and long-term inhibition of $K_v1.3$ channels in T cells. The suppression of $K_v1.3$ was suggested to be associated with the hypoxic inhibition of TCR-mediated proliferation (Conforti et al., 2003). The unique hypoxic upregulation of TASK-2 and the augmented Ca^{2+} signals by hyperpolarization might contribute to the positive regulation of B cell responses.

Conclusion

In summary, the expression of TASK-2 was firstly identified in B lymphocytes. In the B lymphocytes (WEHI-231), the

expression of TASK-2 is dramatically increased by 12 h BCR-ligation mediated by Ca^{2+}/calcineurin signalling pathway, and this response might be putatively associated with apoptosis. In addition, the expression of TASK-2 in WEHI-231 is markedly upregulated by hypoxia in a HIF-1α dependent manner. The augmented Ca^{2+} influx in the SH cells could arise from the enhanced electrical driving force (i.e., hyperpolarizing effect of TASK-2). More rigorous studies about the immunological implication of TASK-2 in systemic levels need to be conducted.

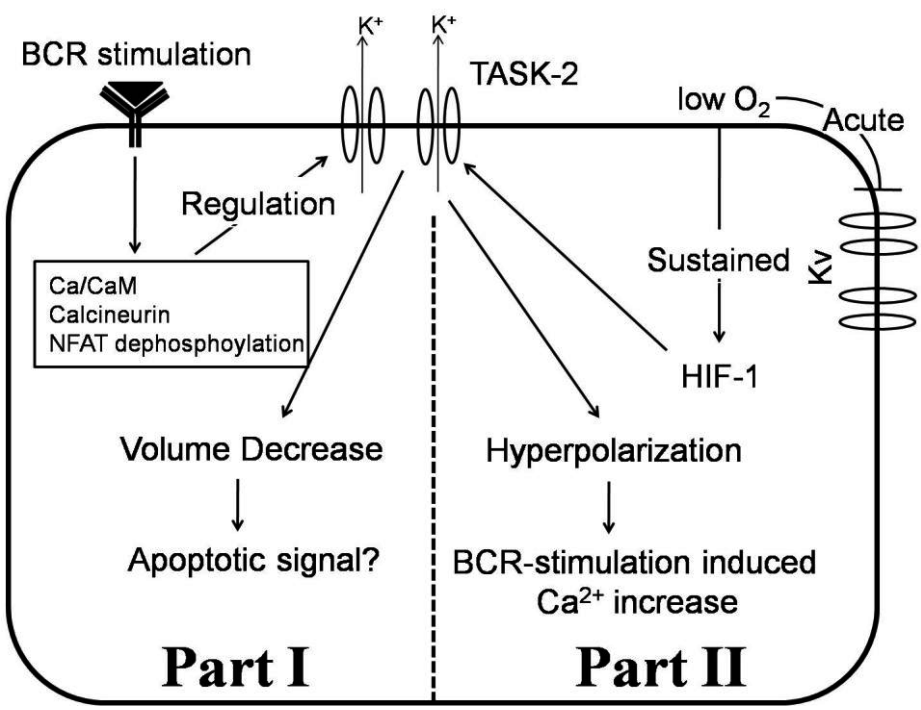

REFERENCES

Archer SL, Wu XC, Thebaud B, Nsair A, Bonnet S, and Tyrrell B. et al. Preferential expression and function of voltage-gated, O_2-sensitive K^+ channels in resistance pulmonary arteries explains regional heterogeneity in hypoxic pulmonary vasoconstriction: ionic diversity in smooth muscle cells. *Circ Res.* 2004 Aug; 95: 308-318.

Atkuri KR, Herzenberg LA, and Herzenberg LA. Culturing at atmospheric oxygen levels impacts lymphocyte function. *Proc Natl Acad Sci USA.* 2005 Mar; 102: 3756-3759.

Bayliss DA, and Barrett PQ. Emerging roles for two-pore-domain potassium channels and their potential therapeutic impact. *Trends Pharmacol Sci.* 2008 Nov; 29: 566-575.

Barriere H, Belfodil R, Rubera I, Tauc M, Lesage F, and Poujeol C. et al. Role of TASK-2 potassium channels regarding volume regulation in primary cultures of mouse proximal tubules. *J Gen Physiol.* 2003 Aug; 122: 177-190.

Beeton C, Wulff H, Standifer NE, and Chandy KG. Kv1.3 channels are a therapeutic target for T cell-mediated autoimmune diseases. *Proc Natl Acad Sci USA.* 2006 Nov; 103: 17414-17419.

Buckler KJ. A novel oxygen-sensitive potassium current in rat carotid body type I cells. *J Physiol.* 1997 Feb; 498: 649-662.

Buckler KJ, Williams BA, and Honore E. An oxygen-, acid- and anaesthetic-sensitive TASK-like background potassium channel in rat arterial chemoreceptor cells. *J Physiol.* 2000 May; 525: 135-142.

Bittner S, Meuth SG, Göbel K, Melzer N, Herrmann AM, and Simon OJ. et al. TASK-1 modulates inflammation and neurodegeneration in autoimmune inflammation of the central nervous system. *Brain.* 2009 Sep; 132: 2501-2516.

Bittner S, Bobak N, Herrmann AM, Göbel K, Meuth P, and Höhn KG. et al. Upregulation of K2P5.1 potassium channels in multiple sclerosis. *Ann Neurol.* 2010 Jul; 68: 58-69.

Bortner CD, and Cidlowski JA. Cell shrinkage and monovalent cation fluxes: role in apoptosis. *Arch Biochem Biophys.* 2007 Jun; 462: 176-188.

Brazier SP, Mason Hs, Bateson AN, and Kemp PJ. Cloning of the human TASK-2 (KCNK5) promoter and its regulation by chronic hypoxia. *Biochem Biophys Res Commun.* 2005 Nov; 336: 1251-1258.

Cahalan MD, and Chandy KG. The functional network of ion channels in T lymphocytes. *Immunol Rev.* 2009 Sep; 231: 59-87.

Caldwell CC, Kojima H, Lukashev D, Armstrong J, Farber M, and Apasov SG. et al. Diffenrential effects of physiologically relevant hypoxic conditions on T lymphocyte development and effector functions. *J Immunol.* 2001 Dec; 167: 6140-6149.

Chimote AA, Kuras Z, and Conforti L. Disruption of kv1.3 channel forward vesicular trafficking by hypoxia in human T

lymphocytes. *J Biol Chem.* 2012 Jan; 287: 2055-2067.

Cho SY, Beckett EA, Baker SA, Han I, Park KJ, and Monaghan K. et al. A pH-sensitive potassium conductance (TASK) and its function in the murine gastrointestinal tract. *J Physiol.* 2005 May; 565: 243-259.

Chung SC, Limnander A, Kurosaki T, Weiss A, and Korenbrot JI. Coupling Ca^{2+} store release to I_{crac} channel activation in B lymphocytes requires the activity of Lyn and Syk kinases. *J Cell Biol.* 2007 Apr; 177: 317-328.

Conforti L, Petrovic M, Mohammad D, Lee S, Ma Q, Barone S, and Filipovich AH. Hypoxia regulates expression and activity of Kv1.3 channels in T lymphocytes: a possible role in T cell proliferation. *J Immunol.* 2003 Jan; 170: 695-702.

Cotton JF, Zou HL, Liu C, Au JD, and Yost CS. Identification of native rat cerebellar granule cell currents due to background K channel KCNK5 (TASK-2). *Brain Res Mol Brain Res.* 2004 Sep; 128: 112-120.

Donnelly DF, Kim I, Yang D, and Carroll JL. Role of MaxiK-type calcium dependent K^+ channels in rat carotid body hypoxia transduction during postnatal development. *Respir Physiol. Neurobiol.* 2011 Jun; 177: 1-8.

Duprat F, Girard C, Jarretou G, and Lazdunski M. Pancreatic two P domain K^+ channels TALK-1 and TALK-2 are activated by nitric oxide and reactive oxygen species. *J Physiol.* 2005 Jan; 562: 235-244.

Duprat F, Lauritzen I, Patel A, and Honoré E. The TASK background K2P channels: chemo- and nutrient sensors. *Trends Neurosci.* 2007 Nov; 30: 573-580.

Eeva J, and Pelkonen J. Mechanisms of B cell receptor induced apoptosis. *Apoptosis.* 2004 Sep; 9: 525-531.

Gabriel A, Abdallah M, Yost CS, Winegar BD, and Kindler CH. Localization of the tandem pore domain K^+ channel KCNK5 (TASK-2) in the rat central nervous system. *Brain Res Mol Brain Res.* 2002 Jan; 98: 153-163.

Gestreau C, Heitzmann D, Thomas J, Dubreuil V, Bandulik S, and Reichold M. et al. TASK-2 potassium channels set central respiratory CO_2 and O_2 sensitivity. *Proc Natl Acad Sci USA.* 2010 Feb; 107: 2325-2330.

Gurney A M, Osipenko ON, MacMillan D, McFarlane KM, Tate RJ, and Kempsill FE. Two-pore domain K channel, TASK-1, in pulmonary artery smooth muscle cells. *Circ Res.* 2003 Nov; 93: 957-964.

Han J, and Kang D. TRESK channel as a potential target to treat T-cell mediated immune dysfunction. *Biochem Biophys Res Commun.* 2009 Dec; 390: 1102-1105.

Huang JH, Cardenas-Navia LI, Caldwell CC, Plumb TJ, Radu CG, and Rocha PN. et al. Requirements for T Lymphocyte Migration in Explanted Lymph Nodes. *J Immunol.* 2007 Jun; 178: 7747-7755.

Jiang BH, Rue E, Wang GL, Roe R, and Semenza GL. Dimerizaion DNA binding, and transactivation properties of

hypoxia-inducible factor 1. *J Biol Chem.* 1996 Jul; 271: 17771-17778.

Jiang BH, Semenza GL, Leung SW, Passantino R, Concordet JP, and Maire P. et al. Hypoxia response elements in the aldolase A, enolase 1, and lactate dehydrogenase A gene promoters contain essential binding sites for hypoxia-inducible factor 1. *J Biol Chem.* 1996 Dec; 271: 32529-32537.

Kim D. Physiology and pharmacology of two-pore domain potassium channels. *Curr Pharm Des.* 2005 11: 2717-2736.

Kirkegaard SS, Lambert IH, Gammeltoft S, and Hoffmann EK. Activation of the TASK-2 channel after cell swelling is dependent on tyrosine phosphorylation. *Am J Physiol Cell Physiol.* 2010 Oct; 299: C844-853.

Kojima H, Gu H, Nomura S, Caldwell CC, Kobata T, and Carmeliet P. Abnormal B lymphocyte development and autoimmunity in hypoxia-inducible factor 1alpha-deficient chimeric mice. *Proc Natl Acad Sci USA.* 2002 Feb; 99: 2170-

2174.

Kuppers R, Klein U, and Hansmann ML. Cellular origin of Human B cell lymphomas. *N Engl J Med.* 1999 Nov; 341: 1520-1529.

Kurosaki T. Regulation of B-cell signal transduction by adaptor proteins. *Nat Rev Immunol.* 2002 May; 2: 354-363.

La, JH, Kang D, Park JY, Hong SJ, and Han J. A novel acid-sensitive K^+ channel in rat dorsal root ganglia neurons. *Neurosci Lett.* 2006 Oct; 406: 244-249.

Lambert IH, Pedersen SF, and Poulsen KA. Activation of PLA2 isoforms by cell swelling and ischaemia/hypoxia. *Acta physiol.* 2006 May; 187: 75-85.

Lang F, Huber SM, Szabo I, and Gulbins E. Plasma membrane ion channels in suicidal cell death. *Arch Biochem Biophys.* 2007 Jun; 462: 189-194.

L' Hoste S, Poet M, Duranton C, Belfodil R, Barriere H, and Rubera I. Role of TASK2 in the Control of Apoptotic Volume Decrease in Proximal Kidney Cells. *J Biol Chem.* 2007 Dec; 282: 36692-36703.

Liu QH, Liu X, Wen Z, Hondowicz B, King L, and Monroe J. et al. Distinct calcium channels regulate responses of primary B lymphocytes to B cell receptor engagement and mechanical stimuli. *J Immunol.* 2005 Jan; 174: 68-79.

Lopes CM, Rohacs T, Czirjak G, Balla T, Enyedi P, and Logothetis DE. PIP_2 hydrolysis underlies agonist-induced inhibition and regulates voltage gating of two-pore domain K^+ channels. *J Physiol.* 2005 Apr; 564: 117-129.

Loeffler DA, Juneau PL, and Masserant S. Influence of tumour physico-chemical conditions on interleukin-2-stimulated lymphocyte proliferation. *Br J Cancer.* 1992 Oct; 66: 619-622.

Lotshaw DP. Biophysical, pharmacological, and functional characteristics of cloned and native mammalian two-pore

domain K^+ channels. *Cell Biochem Biophys.* 2007 47: 209-256.

Mancino A, Schinoppa T, Larghi P, Pasqualini F, Nebuloni M, and Chen IH. Divergent effects of hypoxia on dendritic cell functions. *Blood.* 2008 Nov; 112: 3723-3734.

McNamee E, Korns Johnson ND, Homann D, and Clambey ET. Hypoxia and hypoxia-inducible factors as regulators of T cell development, differentiation, and function. *Immunol Res.* 2013 Mar; 55: 58-70.

Meuth SG, Bittner S, Meuth P, Simon OJ, Budde T, and Wiendl H. TWIK related acid-sensitive K^+ channel TASK-1 and TASK-3 critically influence T lymphocyte effector functions. *J Biol Chem.* 2008 May; 283:14559-14570.

Miller P, Kemp PJ, Lewis A, Chapman CG, Meadows HJ, and Peers C. Acute hypoxia occludes hTREK-1 modulation: re-evaluation of the potential role of tandem P domain K^+ channels in central neuroprotection. *J Physiol.* 2003 Apr; 548: 31-37.

Morton MJ, O'Connell AD, Sivaprasadarao A, and Hunter M. Determinants of pH sensing in the two-pore domain K^+ channel, TASK-2. *Pflugers Arch.* 2003 Feb; 102: 16102-16106.

Nam JH, Woo JE, Uhm DY, and Kim SJ. Membrane-delimited regulation of novel background K^+ channels by MgATP in murine immature B cells. *J Biol Chem.* 2004 May; 279: 20643-20654.

Nam JH, Lee HS, Nguyen YH, Kang TM, Lee SW, and Kim HY et al. Mechanosensitive activation of K^+ channel via phospholipase C-induced depletion of phosphatidylinositol 4,5-bisphosphate in B lymphocytes. *J Physiol.* 2007 Aug; 582: 977-990.

Nam, JH, Shin DH, Zheng H, Lee DS, Park SJ, and Park KS et al. Expression of TASK-2 and its upregulation by B cell receptor stimulation in WEHI-231 mouse immature B cells. *Am J Physiol Cell Physiol.* 2011 Feb; 300: C1013-1022.

Neumann AK. Yang J, Biju MP, Joseph SK, Jphnson RS, and

Haase VH. Hypoxia inducible factor1 alpha regulates T cell receptor signal transduction. *Proc Natl Acad Sci USA.* 2005 Nov; 102: 17071-17076.

Niemeyer MI, Cid LP, Barros F, and Sepulveda FV. Modulation of two-pore domain acid-sensitive K^+ channel TASK-2 (KCNK5) by changes in cell volume. *J Biol Chem.* 2001 Nov; 276: 43166-43174.

Nizet V, and Johnson RS. Interdependence of hypoxic and innate immune response. *Nat Rev Immunol.* 2009 9: 609-617.

Overholt JL, Ficker E, Yang T, Shams H, Bright GR, and Prabhakar NR. HERG-Like potassium current regulates the resting membrane potential in glomus cells of the rabbit carotid body. *J Neurophysiol.* 2000 May; 83: 1150-1157.

Palazon A, Aragones J, Morales-Kastresana A, de Landazuri MO, and Melero I. Molecular pathways: hypoxia response in immune cells fighting or promoting cancer. *Clin Cancer Res.* 2012 May; 18: 1207-1213.

Patel AJ, and Lazdunski M. The 2P-domain K^+ channels: role in apoptosis and tumorigenesis. *Pflugers Arch.* 2004 Jun; 448: 261-273.

Peers C. Hypoxic suppression of K^+ currents in type I carotid body cells: selective effect on the Ca^{2+}-activated K^+ current. *Neurosci Lett.* 1990 Nov; 119: 253-256.

Reyes R, Duprat F, Lesage F, Fink M, Salinas M, and Farman N. et al. Cloning and expression of a novel pH-sensitive two pore domain K^+ channel from human kidney. *J Biol Chem.* 1998 Nov; 273: 30863-30869.

Platoshyn O, Yu Y, Golovina VA, McDaniel SS, Krick S, and Li L. et al. Chronic hypoxia decreases K_v channel expression and function in pulmonary artery myocytes. *Am J Physiol Lung Cell Mol Physiol.* 20010 Apr; 280: L801-812.

Pottosin II, Bonales-Alatorre E, Valencia-Cruz G, Mendoza-Magana ML, and Dobrovinskaya OR. TRESK-like potassium

channels in leukemic T cells. *Pflugers Arch.* 2008 Sep; 456: 1037-1048.

Scharenberg AM, Humphries LA, and Rawlings DJ. Calcium signalling and cell-fate choice in B cells. *Nat Rev Immunol.* 2007 Oct; 7: 778-789.

Semenza, GL, Jiang BH, Leung SW, Passantino R, Concordet JP, Maire P, and Giallongo A. Hypoxia response elements in the aldolase A, enolase 1, and lactate dehydrogenase A gene promoters contain essential binding sites for hypoxia-inducible factor 1. *J Biol Chem.* 1996 271: 32529-32537.

Singh I, Chohan IS, Lai M, Khanna PK, Srivastava MC, and Nanda RB. et al. Effects of high altitude stay on the incidence of common diseases in man. *Int J Biometeorol.* 1977 Jun; 21: 93-122.

Sluimer JC, Gasc JM, van Wanroij JL, Kisters N, Groeneweg M, and Sollewijn Gelpke MD. et al. Hypoxia, hypoxia-inducible

transcription factor, and macrophages in human atherosclerotic plaques are correlated with intraplaque angiogenesis. *J Am Coll Cardiol.* 2008 Apr; 51: 1258-1265.

Szigligeti P, Neumeier L, Duke E, Chougnet C, Takimoto K, and Lee SM. et al. Signalling during hypoxia in human T lymphocytes critical role of the src protein tyrosine kinase p56Lck in the O_2 sensitivity of $K_v1.3$ channels. *J Physiol.* 2006 Jun; 573: 357-370.

Trimarchi JR, Liu L, Smith PJ, and Keefe DL. Apoptosis recruits two-pore domain potassium channels used for homeostatic volume regulation. *Am J Physiol Cell Physiol.* 2002 Mar; 282: C588-C594.

Wang GL, Jiang BH, Rue EA, and Semenza GL. Hypoxia-inducible factor 1 is a basic-helix-loop-helix-PAS heterodimer regulated by cellular O_2 tension. *Proc Natl Acad Sci USA.* 1995 Jun; 92: 5510-5514.

Warth R, Barriere H, Meneton P, Bloch M, Thomas J, and Tauc

M. et al. Proximal renal tubular acidosis in TASK2 K^+ channel–deficient mice reveals a mechanism for stabilizing bicarbonate transport. *Proc Natl Acad Sci USA.* 2004 May; 101: 8215–8220.

Wyatt CN, Wright C, Bee D, and Peers E. O_2–sensitive K^+ currents in carotid body chemoreceptor cells from normoxic and chronically hypoxic rats and their roles in hypoxic chemotransduction. *Proc Natl Acad Sci USA.* 1995 Jan; 92: 295–299.

Wulff H, Knaus HG, Pennington M, and George Chandy KG. K^+ channel expression during B cell differentiation: implications for immunomodulation and autoimmunity. *J Immunol.* 2004 Jul; 173: 776–786.

Yeo EJ, Chun YS, Cho YS, Kim J, Lee JC, and Kim MS. et al. YC–1: a potential anticancer drug targeting hypoxia–inducible factor 1. *J Natl Cancer Inst.* 2003 Apr; 95: 516–525.

Yeo EJ, Ryu JH, Cho YS, Chun YS, Huang LE, and Kim MS. et al. Amphotericin B blunts erythropoietin response to hypoxia by reinforcing FIH-mediated repression of HIF-1. *Blood.* 2006 Feb; 107: 916-923.

Zheng H, Nam JH, Nguen YH, Kang TM, Kim TJ, and Earm YE. et al. Arachidonic acid-induced activation of large-conductance potassium channels and membrane hyperpolarization in mouse B cells. *Pflugers Arch.* 2008 Aug; 456: 867-881.

Zheng H, Nam JH, Pang B, Shin DH, Kim JS, and Chun YS. et al. Identification of the large-conductance background K^+ channel in mouse B cell as TREK-2. *Am J Physiol Cell Physiol.* 2009 Jul; 297: C188-C197.

Zuckerberg AL, Goldberg LI, and Lederman HM. Effects of hypoxia on interleukin-2 mRNA expression by T lymphocytes. *Crit Care Med.* 1994 Feb; 22: 197-203.

국문 초록

미성숙 B 림프구는 수용체 자극에 의하여 세포자멸사를 겪게 되는데, 이는 '자기반응적' 인 세포를 제거하는 것이다. B 림프구는 생리학적 저산소조건 (1-5% P_{O2})으로 알려진 비장이나 림프절에서 분화하는 것으로 알려져 있다. K^+ 이온통로는 림프구에서 세포자멸사 및 세포용적 등 다양한 역할을 한다. 그러나 B 림프구의 수용체 자극과 저산소와 관련된 포타슘 이온통로의 연구는 아직 알려져 있지 않다. 본 연구에서 생쥐 B 림프구 수용체자극 후 24시간 후에 증가하는 전압비의존적 background K^+ 전도도의 증가를 확인하였다. 이것의 생물리학적특성 (pH 민감도, 단일전도도) 은 two-pore domain K^+ (K2P) family 중 TASK-2 와 유사한 것을 확인하였다. B 림프구 수용체 자극후 증가하는 K^+ 이온전류는 면역블로팅방법과 역전사 중합효소반응, 그리고 특이적 siTASK-2 실험결과 TASK-2 이온통로로 확인되었고, 이는 calcineurin 억제제 (cyclosporine A 또는 FK506)에 의하여 그 증가가 나타나지 않았다. WEHI-231 세포수용체 자극 후 일어나는 세포사멸은 siTASK-2에 의하여 줄어들었고, 생쥐 비장에서 분리한 B 림프구에서 TASK-2 의 활성과 mRNA 를 확인하였다.

B 림프구 수용체 자극뿐만 아니라 저산소 (3%, P_{O2}) 에 노출된

WEHI-231 세포는 TASK-2 이온통로의 증가를 보였다. 이러한 이온통로의 증가는 20 시간 이후부터 48 시간까지 지속적 나타났다. 이러한 이온통로의 증가는 HIF-1α 억제제로 알려진 YC-1 전 처리와 특이적 siHIF-1α 에 의하여 차단되었다. 또한 대기중 산소 농도에서도 HIF-1α 를 안정화 시킬 수 있는 sh-HIF-1α 를 WEHI-231 세포에 발현시킨 후 TASK-2 전류를 확인하였다. 저산소에 노출된 WEHI-231 세포는 TASK-2 이온통로의 증가를 보이고, 이는 수용체 자극에 의한 세포내 Ca^{2+} 의 증가를 보인다. 저산소에 의한 TASK-2 이온통로의 증가는 비장유래 생쥐 B 림프구에서도 관찰되었다.

본 연구를 요약하면 B 림프구 수용체 자극과 저산소에 의하여 TASK-2 이온통로의 증가를 보이며, 이는 자극원에 따라 다양한 역할을 할 것으로 기대된다. B 림프구 수용체 자극에 의하여 TASK-2 이온통로의 증가는 과다한 K^+ 이온유출을 일으키게 되고, 이는 세포막을 과분극 시킬 것이다. 이 결과 세포사멸시 보이는 세포용적 감소에 기여를 할 것이다. 반면에 저산소로 유발된 TASK-2 이온통로의 경우 세포내 Ca^{2+} 을 증가시키게 되고, 이는 B 림프구의 활성과 세포운명을 결정할 것이다.

본 논문 Part I 은 *Am J Physiol Cell Physiol.* Nam and Shin et al., 2011 에 출판된 논문이며, Part II 는 현재 저널 투고 예정임.

주요어 : B 림프구, TASK-2 이온통로, 저산소, B 세포수용체 자극
학 번 : 2008-21944